3065

70

DISTRIBUTION STATEMENT A
Approved for Public Release
Distribution Unlimited

R and D CENTER
LABORATORY
TECHNICAL REPORT

NO. 12573

PART II

FORMATION AND FAILURE OF ELASTOMER NETWORKS VIA THERMAL, MECHANICAL AND SURFACE CHARACTERIZATION

CONTRACT NO. DAAK30-78-C-0098

DECEMBER, 1980

by DAVID W. DWIGHT, J. E. McGRATH & R. M. YANG

DEPARTMENT OF MATERIALS ENGINEERING and
DEPARTMENT OF CHEMISTRY
VIRGINIA POLYTECHNIC INSTITUTE AND STATE
UNIVERSITY BLACKSBURG, VIRGINIA 24060

Distribution
Unlimited

U.S. ARMY TANK-AUTOMOTIVE COMMAND
RESEARCH AND DEVELOPMENT CENTER
Warren, Michigan 48090

REPORT DOCUMENTATION PAGE

READ INSTRUCTIONS BEFORE COMPLETING FORM

1. REPORT NUMBER: 12573	2. GOVT ACCESSION NO.
3. RECIPIENT'S CATALOG NUMBER	
4. TITLE (and Subtitle): Formation and Failure of Elastomer Networks *via* Thermal, Mechanical and Surface Characterization	5. TYPE OF REPORT & PERIOD COVERED: Final Technical Report July 1, 1980 - Dec.31, 1980
	6. PERFORMING ORG. REPORT NUMBER
7. AUTHOR(s): David W. Dwight and James E. McGrath and Ray M. Yang	8. CONTRACT OR GRANT NUMBER(s): DAAK30-78-C-0098
9. PERFORMING ORGANIZATION NAME AND ADDRESS: Department of Materials Engineering and Chemistry, Virginia Polytechnic Institute and State University, Blacksburg, VA 24061	10. PROGRAM ELEMENT, PROJECT, TASK AREA & WORK UNIT NUMBERS: CMS 612601.H 910011
11. CONTROLLING OFFICE NAME AND ADDRESS: U. S. Army Tank-Automotive Command, Warren, MI 48090	12. REPORT DATE: May 1981
	13. NUMBER OF PAGES: 95
14. MONITORING AGENCY NAME & ADDRESS(if different from Controlling Office)	15. SECURITY CLASS. (of this report): UNCLASSIFIED
	15a. DECLASSIFICATION/DOWNGRADING SCHEDULE

16. DISTRIBUTION STATEMENT (of this Report)
Distribution Unlimited.

17. DISTRIBUTION STATEMENT (of the abstract entered in Block 20, if different from Report)

18. SUPPLEMENTARY NOTES

19. KEY WORDS (Continue on reverse side if necessary and identify by block number)

Oxygen to Carbon Ratio (O/C)
crosslink density
% weight loss
volatile, glass transition temperature
TGA, TMA
ESCA SEM/EDAX

20. ABSTRACT (Continue on reverse side if necessary and identify by block number)

Systematic study of tank track pads tested on paved, cross-country, and gravel courses was done with respect to the change in thermal, surface and mechanical properties. Experimental measurements were conducted mostly on paved course pads of different service mileage and manufacturers.

ESCA was utilized to monitor the oxidative degradation casued by road service. In most cases, oxygen to carbon ratio (O/C) was found to increase with increasing service mileage. Solvent extracted samples show clearly the pad surface contains more oxygen than the bulk. SEM/EDXA identifies not only the

20.

nature of failure initiation sites but also the morphology of service-pad surface and bulk. Swelling experiment shows crosslink density changes with service life for thin-surface samples, but no changes for thick samples. The evidence accumulated from ESCA, SEM and swelling suggests strongly that the oxidative crosslinking reaction takes place primarily at the pad surface. Within 1mm from the surface, the composition is similar to the original bulk.

Thermal property changes are experimentally less pronounced in magnitude. Nevertheless, volatile content from TGA, and glass transition temperature (T_g) from TMA do correlate quite well with the O/C ratio from ESCA. It seems certain that the oxidation plays a role in restricting the molecular mobility, while the volatile moieties act as plasticizers. Cross-country pads tested show that T_g for crack surfaces is generally higher than at wear sites. This observation supports our model of crack propagation through an embrittled matrix.

Statistical field test data indicate the % weight loss per 250 miles of service is 4 to 8% on paved course, 8 to 15% on gravel and 30 to 45% in cross-country service. The visual appearance of failed pads is also quite different in cross-country than in paved course. Terrain penetration and chunk tearing are more apparent and severe in cross-country pads while the mechanism for weight loss in paved course pads is mainly due to abrasive wear.

FINAL REPORT

PART II

FORMATION AND FAILURE OF ELASTOMER NETWORKS VIA THERMAL, MECHANICAL AND SURFACE CHARACTERIZATION

by

David W. Dwight, James E. McGrath, and Ray M. Yang

prepared for

Department of the Army
Contract DAAK30-78-C-0098

March, 1981

U.S. Army Tank-Automotive Research and Development Command
Warren, Michigan 48090
Mr. Jacob Patt

Department of Materials Engineering and
Department of Chemistry

Virginia Polytechnic Institute and State University
Blacksburg, Virginia 24061

TABLE OF CONTENTS

1. INTRODUCTION

This report will focus on our systematic study of experimental track pads tested on paved, cross-country, and gravel courses at the Yuma Proving Grounds (YPG). The post-service pads, each one from a different course, mileage and manufacturer, were provided through the help of Mr. Jacob Patt at TARADCOM. Track pads were manufactured by Goodyear, Firestone, Standard Products, and Monarch. Data on weight of track pads vs test mileage at YGP were provided by Mr. Patt.

T142 pads are approximately 11 inches long, 4 inches wide and 2 inches thick. They meet the current standard as written in Military Specification (mil spec), MIL-T-11891B. Acceptable values of physical properties (e.g., hardness, tear resistance, ultimate tensile strength, ozone and aging resistance) are given in the mil spec. The test procedures are stated in the Federal Test Method Standard No. 601. Also, a road test of the pads is required per the mil spec. The service life of pads is expected to be at least 2,000 miles.

The problems of premature tank track pad failure and the rapid wear of track pad elastomers in road service were approached by thermal, mechanical, and surface analyses to determine failure mechanisms and appropriate characterization methods that will ultimately result in the development of better elastomeric materials.

So far, the samples we have received and investigated are:

a. Preservice: There are eight-T142 preservice pads from four manufacturers. Two pads were made by the Goodyear Rubber Company, one made of styrene-butadiene rubber (SBR), the other of SBR blended with chopped Kevlar

fibers. They are designated as GS-0 and GK-0, respectively. Four pads were from the Firestone Rubber Company, one of SBR, one of SBR blended with Kevlar fibers, one made of rubber which is the triblend of SBR, butyl rubber (BR) and natural rubber (NR), the other termed as experimental. They are designated with FS-0, FK-0, FA-0 and FM-0, respectively. The other two SBR pads by Standard Products and Monarch Rubber Companies are coded as SP-0 and MK-0, respectively.

b. Paved: There are 24 pads, 8 each from one of three mileages (500, 1,000, 1,500). To designate these pads, P-mileage is added following the pad type. For example, a Goodyear Kevlar filled SBR pad of 500 miles on paved course is coded GK-P-500.

c. Cross-Country: There are 16 pads, 9 pads of 250 miles service and 7 pads of 366 mile service. The additional 250 mile pad is a pad made by Firestone consisting of triblend of SBR, NR and BR and designated as FA-XC-250. Monarch pads were not included in the 366 mile samples. The designation for cross-country pads is the same as the previous, e.g., FS-XC-366 used to represent Firestone SBR pad of 366 mile service. Noticeably, the overall rate of wear in cross-country service is much more rapid than that of paved course. At 366 miles the field test had to be terminated because the pads were no longer serviceable.

d. Gravel: We received only 8 pads of gravel course service, all after 1,000 miles field testing. The gravel course seems to cause medium wear in track pads since the service life is between the paved and the cross-country pads for the same extent of wear. The preservice pad designation is followed by -G-1000 to identify the individual gravel pad. One of the eight pads received is a T97E2 pad. This is an experimental pad of different design to test the effect of shoe and pad geometry on rubber wear. Photographs for

one pad in each case (a to d) are shown in Figures 1 and 2. The failure mode between test courses is visually different. Rubber wear seems to be the main mechanism of service weight loss on pavement. Chunk failure dominated in cross-country course and the gravel course pads show both types of failure.

The types of experiments and analyses we have carried out are grouped in the areas to which they pertain as follows:

1. Structure-property Relations
    a. Swelling
    b. Modulus by compression stress-strain measurement
2. Thermal Properties
    a. Thermogravimetric Analysis (TGA)
    b. Thermomechanical Analysis (TMA)
3. Surface Analysis
    a. Scanning Electron Microscopy/Energy Dispersive X-ray Analysis (SEM/EDXA) fractography, wear morphology and chemical point anaylsis
    b. Electron Spectroscopy for Chemical Analysis (ESCA) surface chemistry
4. Field weight loss

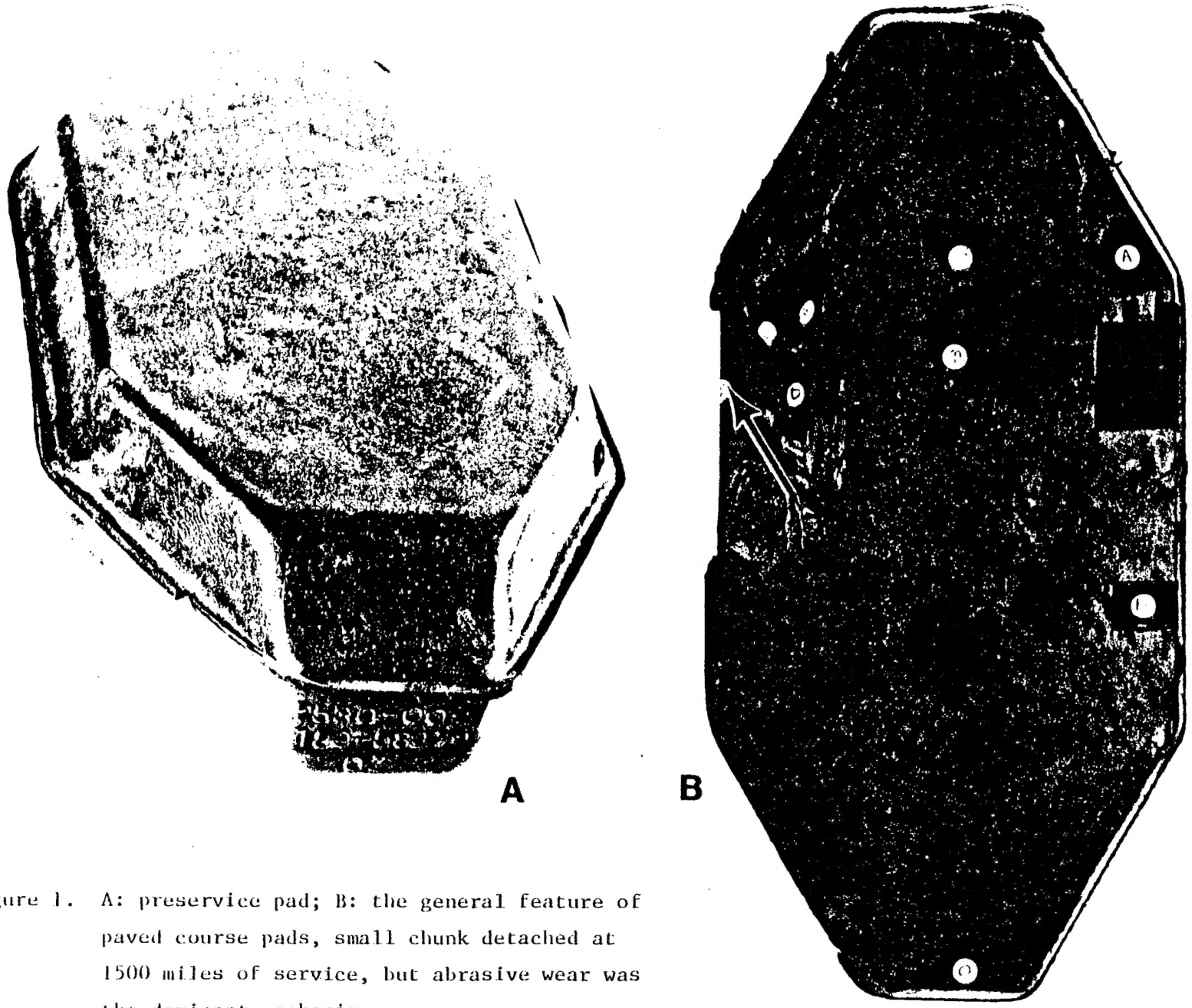

Figure 1. A: preservice pad; B: the general feature of paved course pads, small chunk detached at 1500 miles of service, but abrasive wear was the dominant mechanism.

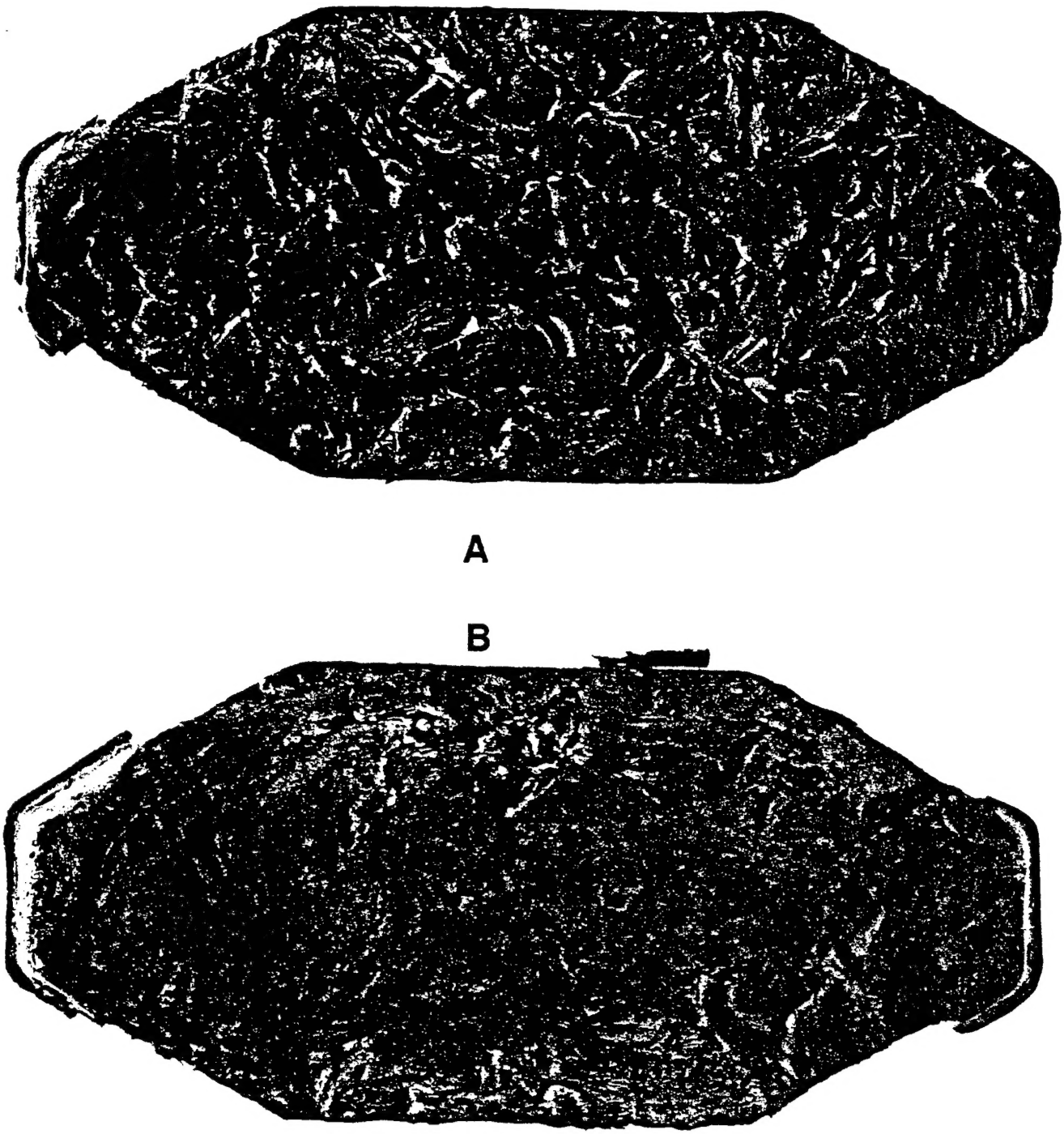

Figure 2. A: the general features of cross country pads, penetration and tearing from terrain are more apparent and severe; B: gravel course pad, fracture mechanisms seem to be variable.

2. SUMMARY

1. Pads were manufactured by four companies: Goodyear, Firestone, Monarch, and Standard Products. Wear rate in tank service was determined on paved, gravel and cross-country courses at Yuma Proving Ground (YPG), AZ.
2. Statistical sampling from the Yuma Proving Grounds field tests is very costly due to the number of different external variables (4 manufacturers, 5 generic compositions, 3 test courses, 4 mileages), as well as the fact that a single sample usually shows at least three levels of compositional heterogeniety both laterally across the pad surface and vertically (in the millimeter depth range). Now, considering that our objective is to develop correlations between the above variables and the results of detailed atomic-molecular/morphological analysis using several modern research techniques, a prohibitively large number of tests is necessary. For these reasons, we focused most of our attention on SBR compositions from three suppliers, after testing on the paved course.
3. Changes in crosslink density were determined from both swelling and modulus measurements, volatile content by TGA, T_g and Tvf by TMA.
4. The physical and chemical nature of the surface and bulk of track pads were determined with the analysis combination of SEM/EDXA and ESCA.
5. Goodyear preservice pads have the highest crosslink density, Standard Product pads second, and Firestone samples have the lowest crosslink density.
6. Relative crosslink density increased after cross-country service.
7. Compressive stress-strain curve is highly sensitive to load, sample surface and thickness, and composition variation. After service, the center of the pad has lower modulus than either the adhesive surface or the wear surface.

8. Using % weight loss at 400°C as a TGA index, the trend of volatile content in wear portion of cross-country pads is always higher than in crack portions. No trend was obvious on the paved course.
9. Generally, T_g increases and Tvf decreases with service life on both paved and cross-country courses. Also, the wear surface of cross-country pad had lower T_g than the crack surface.
10. TGA volatile content, T_g, ESCA O/C ratio and service mileage seem to show consistent trends, at least for a specific sample.
11. SBR oxidizes at 155°C with a heating rate of 20°C/minute.
12. Degradation products and concentrations of ZnO particles and sulfur were found at different fracture initiation sites.
13. Comparison of SEM analyses before and after service and extraction, shows subservice morphology changes have taken place due to the mechanical action of the field test; it is more pronounced on wear than crack surfaces.
14. ESCA indicates the O/C ratio of the surface is several times higher than the pad interior . Generally the O/C ratio increases with service mileage.
15. Statistical data from the YPG tests reveal the service weight loss data generally fall into two groups which may represent the outside and the inside of the track.
16. For T142 pads, FM pads perform best, and while MK pads the poorest on cross-country and gravel courses.
17. For T97E2 pads, service weight loss is between the average and the best T142 pads.

3. CONCLUSIONS

1. High relative crosslink density was observed in the higher service weight loss pads. High crosslink density means a more brittle rubber matrix (lower the extensibility of the molecular chains), and perhaps more prone to tear and wear in service. Differences in crosslinking may affect the service life in a similar fashion.
2. T_g increasing and Tvf decreasing with service life means that the rubbery plateau is shrinking. The addition of diluent has been known to shorten the plateau, and the reduction of the molecular weight to a value less than the molecular weight between entanglements, M_e, will make the plateau disappear.
3. The ESCA O/C ratio increase with service mileage in the insoluble network, but not in the extractables, supports a model with oxidative crosslinking and chain scission leading to low molecular weight hydrocarbons.
4. EDXA of brittle fracture regions revealed high sulfur concentrations. It is reasonable to propose that small regions of high sulfur concentration would lead to a brittle area.
5. ESCA indicates matrix oxidation matrix (highO/C ratio); swelling and TMA show increases in crosslink density at surfaces; SEM reveals surface mechanical wear morphology and debris particles. These areas may be less resistant to crack propagation.
6. The pads positioned on the outside of tank tracks suffer larger weight loss due to more severe mechanical action.
7. The T97E2 pads with different geometry actually show no particular advantage in wear resistence although they are designed for that purpose. Their field weight losses were between the average and the best T142 pads.

8. Firestone Experimental (FM) pads consistently show the lowest weight loss and Monarch (MK) pads have the highest weight loss. On the paved course, Firestone (FT) pads show the highest weight loss.

4. RESULTS & DISCUSSION

4-1 Swelling

The results from the swelling experiment indicate the relative amount of solvent swollen in rubber matrix does not change upon paved course service. This may reflect both the chain scission and the crosslink reaction took place concurrently. Also in the swelling test, we worked with samples of 3-5 mm in thickness which might not be sensitive to crosslinks that were confined to the outer surface. Recent results with thin (~0.2 mm) samples confirms the increase in crosslink density with service life.

Priority specimens were FS, GA, and SP, and only the paved course gave reproducible analytical data. Most of the results are from this set of examples. The swelling results show Goodyear pads with highest crosslink density among all, Standard Product pads second and Firestone samples with lowest crosslink density.

Swelling results did show large differences between pad types and after cross-country service. For the six samples we have studied, the relative crosslink density, 1/Q, increases after cross-country service for all but the Standard Products pad. Furthermore, those pads with relatively low crosslink density also show low wear in field testing.

4-2 Compressive Modulus

In order to detect the properties of both surface and bulk, we separated the rubber pads from the metal shoes by immersing the whole pad in liquid nitrogen. After about 5 minutes the steel shoe was easily removed with little force and the integrity of the rubber pads was perfectly preserved. The successful removal of rubber pads makes it easy to analyze the thermal or mechanical properties of the rubber matrix at different locations within the pad. The follow-up property test is the compressive compliance test,

utilizing Thermomechanical Analyzer (TMA). Since a flat-tip probe only is available at the present time, the absolute compliance or modulus cannot be obtained. However, the relative values of pads at different service ages or location can be useful in evaluating their relative crosslink density. The preliminary compression stress-strain curves indicated the modulus of rubber matrix in the center of a pad is lower than either surface. This result suggests both surface regions possess higher crosslinking density than the center region.

For this measurement we have encountered some constraints for obtaining reliable results with the Perkin-Elmer TMS-2 in the compression mode. The compression stress was found to increase rapidly with strain even at a value as small as 1%. Also the modulus increases rapidly with sample thickness. Therefore, to avoid inaccurate results, we must use the same sample height, perfectly flat and parallel sides, and keep the compressive load as small as possible. Since the service pad consists of nonsmooth wear and/or crack surfaces in addition to the expected existence of composition in homogeneity, an accurate determination of even the relative compression modulus is expected to be tedious at best and perhaps unsuccessful.

4-3 Thermogravimetric analysis (TGA)

Thermogravimetric analysis on all of the pads received was completed. A total of about 170 TGA thermograms have now been obtained (Tables D-1 to D-7). Percent weight loss at 400°C was used as an index of volatile content. From other indices, the TGA data seem to vary randomly with service mileage. An increasing trend of the volatile content was observed in GK, FK, FT, and FM pads and a decreasing trend in GS and FS pads. Standard Product pads show an increase in volatile content at 500 mile service and then a decrease at 1,500 miles.

GS, FS and SP type pads show consistent trends with service mileage among results from TMA, TGA and ESCA. In comparison, the cross-country pads have greater changes and variability in % weight loss at 400°C. In most cases, the weight loss of wear surfaces is larger than that for crack surfaces (FT pad is the only exception). Generally speaking, the volatile content of the 1,000 mile gravel course and 366 mile cross-country course are similar for the same pad type.

4-4 Thermal Mechanical Analysis (TMA)

With a coupling of a First Derivative computer (FDC) quite consistant results from Thermal Mechanical Analysis (TMA) can be obtained. The recorder traced out both TMA and DTMA (Derivative TMA) thermograms at the same time which provided a quick and accurate assignment to T_g and viscous temperature (Tvf) of each system. Information extracted from the thermogram are: T_g, Tvf, and melting temperature of wax (Tmw). The difference in T_g is quite small, and T_g is about -40°C for all preservice pads. This may indicate either the crosslink density is nearly the same in each pad or other factors, such as plasticer, filler, etc., have compensated the mobility of molecular chains.

The temperature where viscous flow starts is known to increase with increasing molecular weight of uncured polymers. Provided the analogue prevails between uncured and vulcanized systems, Tvf can be used as an index for the molecular weight under investigation. Tvf for most preservice samples is around 230°C, except that of Goodyear pads is 215°C, and that of the Monarch pad is 205°C. After 500 miles of service Tvf drops a few degrees in Goodyear pads, but the decrease is more pronounced in Firestone pads, about ten degrees lower. Presumably, mechanical or thermal scission has taken place in these pads. DTMA also detected the existance of wax (melting point about 50-70°C) on the surface of preservice pads. The proportional modulus-temperature

curves obtained in the penetration (indentation) mode are similar in shape for all pads. The glass transition temperatures obtained from TMA are also found to be 15-20°C higher than the reported value in literature. This has been attributed to the different frequencies of this test compared to dilatometry or low frequency dynamic mechanical test. Other parameters, such as heating rate, load, may affect the T_g measurement.

From the TMA results we found that T_g increases with increasing service mileage, while viscous flow temperatures, Tvf, decreases with service age. The molecular basis for these results is as follows: while testing track pads in a real service condition, the mechanical, cyclic compression and shear will stress the rubber blocks and hence raise their temperature. Both the mechanical and the thermal action will break macromolecules to form macro-radicals. In the presence of radical acceptors, e.g. O_2, mechano-reactions cause a decrease in molecular weight from the original polymer because the active reaction intermediates were intercepted and stabilized. Thus, polymer is prevented from branching and crosslinking. The decrease in Tvf indicates the service conditions did reduce the molecular weight of the original polymer. However, a reduction of molecular mobility is implied by the increase of T_g. This result is due to the increase of crosslink density. As the temperature increases in the course of repeating mechanical action, the oxygen solubility in rubber matrix decreases, and macroradicals therefore undergo either branching or crosslinking reaction.

After reviewing all the TMA data of paved course pads, we found the changes of T_g are quite small, at most 5 degrees. However, at this small range of temperature change a correlation between O/C ratio determined by ESCA and the glass transition temperature by TMA, was found (Figure 3). This indicates GS, FS and SP pads show a similar trend although SP pad behaves

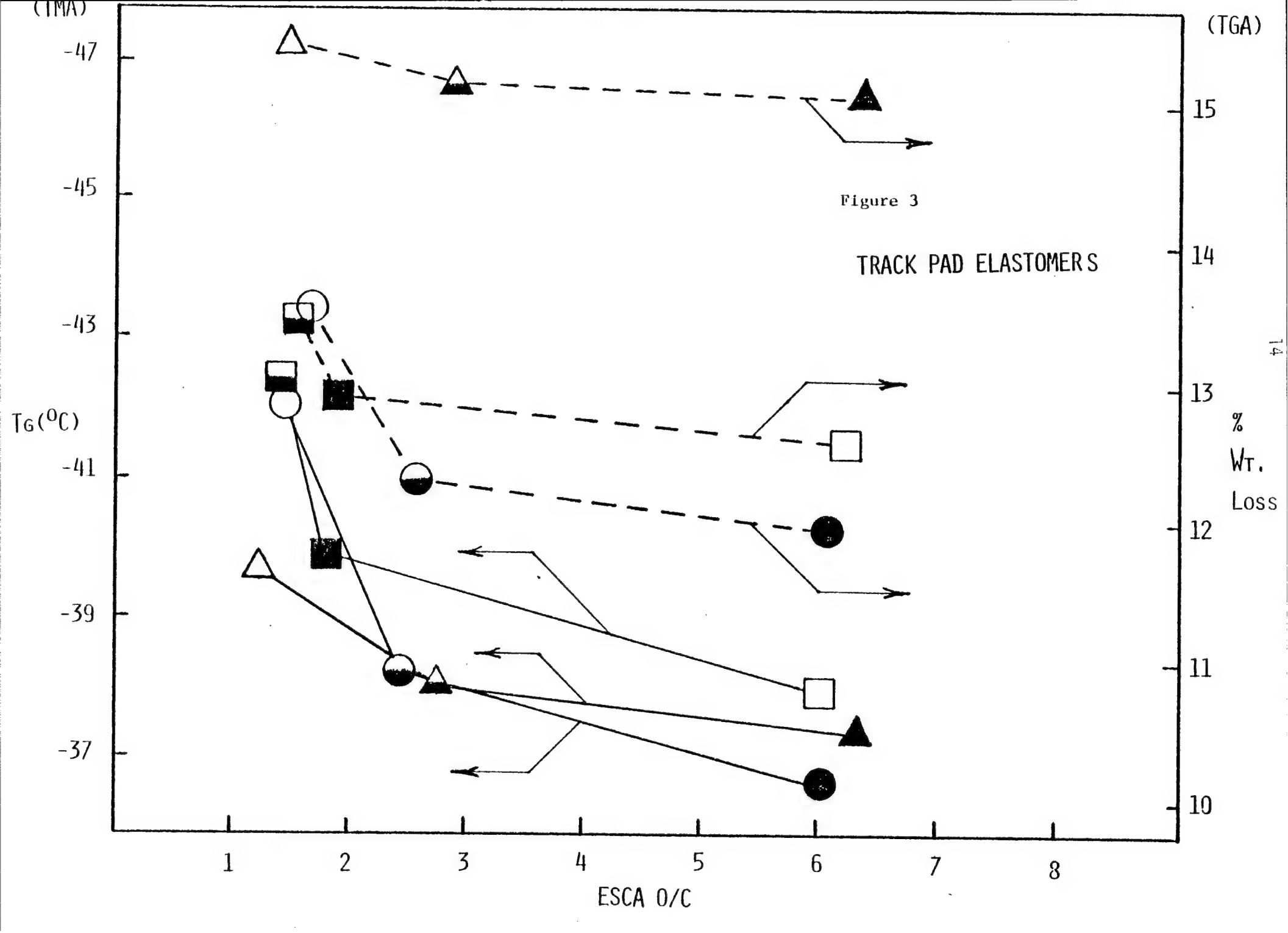
(TMA)
(TGA)
-47
-45
-43
-41
-39
-37
15
14
13
12
11
10
TG(°C)
% Wt. Loss
1
2
3
4
5
6
7
8
ESCA O/C
TRACK PAD ELASTOMERS

Figure 3

differently from FS and GS pads. Thus it seems certain that oxidation plays a role in restricting molecular mobility. In comparison with the TGA % weight loss at 400°C of these pads, another correlation is observed. Higher volatile contents were also found in the pads of lower glass transition temperature as shown in Figure 3.

For the 250 mile cross-country Goodyear Kevlar-filled pad, the fluctuation of glass transition temperature at a crack surface is only ±1°C even with various loads and test pieces (see Table D-8). Larger fluctuation may be expected for specimens from the wear region where the surface is not as smooth as at crack regions. Also, the T_g's of crack surface are higher than those of wear surface with some sporadic exceptions. This tendency is especially true in the case of 250 mile cross country pads. It appears to indicate cracks are likely to propagate through the highly crosslinked matrix. While in the further stage of service (366 mile) as the rubber wear slows, this trend disappears. For FA pads, their T_g's are 10 to 20 degrees lower than other pads, they also perform well in resisting service wear. This may have been the result of lower T_g and better wear resistance of natural rubber to SBR rubber.

4-5 Scanning Electron Microscopy/Energy Dispersive X-ray Analysis (SEM/EDXA)

In previous fractography we observed several types of fracture features and also inhomogeneous blending of zinc oxide particles. Subsequent study of fracture surfaces of the Red River pads was carried out. We found granular fracture surfaces on both wear and crack regions. There were occasional large, vertical cracks, and a large, sharp stone (~ 1 cm in size) imbedded inside a crack more than a centimeter from the outside.

A fairly large amount of Fe appeared in EDXA, and is believed to arise from the soil remaining on the pad surface.

On the SEM/EDXA analysis of the 1,500-mile pavement service pads, we found granulated matrix and inhomogeneities, as observed before on the fracture sites. Details of the fractographs are:

(1) Granulated rubber in the Standard Product pad seems more round than those in Goodyear and Firestone pads;

(2) EDXA spectra indicate more zinc in both Goodyear and Firestone pads than in Standard Product;

(3) Some rod-shaped pointed particles, about 2 μm in length, were observed in the debris. They are similar to "roll-up" particles seen in abrasive wear of elastomers.

(4) There was only one case of "chunking" failure in all pavement specimens. A region of brittle fracture is present at the locus of crack initiation. An extraordinary amount of sulfur found by EDXA in this location corroborates our previous conclusion that inhomogeneity of compounding ingredients promotes fracture initiation in "chunking" failure

The SEM photomicrographs on cross-country pads show wear surface microfeatures similar to pads run on pavement through macrocracking might be different. SEM study of cross sections cut normal to a failure surface indicates that microcracks and granular features exist only near the surface and do not extend into the bulk of the pad.

SEM photographs of cross-country pads show that the granular microfeatures of wear surfaces are pretty much the same as that of crack surfaces, although macroscopically they may loook different. For the cross section cut normal to pad surface we observe regions of different brightness at wear portions. There is an indication that the near-surface region is beginning to granulate, additional surfaces cut normal to wear and crack portions and on parallel sections just beneath those surfaces were studied by

SEM. We observed that most of the surface of different brightness regions were on the worn surface or on the underlayer of the pad surface. Composition and density variations were assessed using EDXA chemical point-analysis. These results help explain the observed appearance of those different regions. The technique is very successful in discriminating among particles derived from the terrain, rubber-fragments, and compounding ingredients. Zinc oxide particles and the rubber-wear debris mechanical comminution are found to correlate closely with the occurance of different brightness sub-surface patches. The zinc oxide particles were located at the center of circular, dark regions in many instances, while other patches did not show this phenomenon.

The morphology seen with SEM changes with swelling, appearing clean and free of debris. EDXA also confirms these extracted surfaces are indeed rubber and free of terrain contamination. Although we were unable to indentify zinc oxide particles, more Zn and S were observed in the EDXA spectra. The swollen and dried bulk sometimes looks different than unswollen. In one case, small cracks and voids were found throughout the examined surface of Standard Products pad.

EDXA indicates particles deposited on cut surfaces possibly consist of terrain particles, clay fillers, compounding particles such as zinc oxide, as well as rubber granules. Sulfur was uniformly dispersed (no high sulfur region was found) while zinc oxide was not. Since EDXA is limited to about 1 μm into the subsurface, the chemical composition characterization of heavily contaminated outer surface is generally not very reliable.

4-6 Electron Spectroscopy for Chemical Analysis (ESCA)

We have performed ESCA analysis selecting three different surfaces, (1) bulk surface cross sectioned with a razor blade, (2) outside surface as

received, and (3) outside surface cleaned with acetone in order to remove dust, wax, or grease. The silicon content on the cleaned surface is much lower than in the other two. Perhaps acetone removes the moiety containing silicon, such as siloxane mold release agent. Also the carbon peak of the cleaned surface is a clear doublet, one component from hydrocarbon groups and one from CO_x or N_yCO_x groups. We also noticed nitrogen on the cleaned surface, but there was no nitrogen in the bulk sample. Generally speaking, pad surface always contains more oxygen than bulk cross section. This is understandable since the surface has been exposed to air over a long period of time and reaction with oxygen is not avoidable. Some pads showed higher oxygen in the bulk, apparently due to the surface being covered with a layer of wax. In such cases, when the surface of the waxy materials was cleaned in order to obtain ESCA information of rubber matrix, then the results agree with the general trend mentioned above.

Comparing the O/C ratio determined by ESCA in different service conditions we found an increase with service age for FS and GS. At 1500 miles the O/C ratio increased 4.7 times in the Goodyear samples and 3.4 times in the Firestone samples. However, Standard Products behaves differently in both O/C ratio and glass transition temperature. Perhaps this is related to microwave vs thermal vulcanization. The surface contains more oxygen than bulk does.

The findings in pavement pads are summarized below:

(1) The bulk cross sections in both failure and wear regions show the same O/C ratio, averaging 5.8% on failure regions, and 6.7% on wear regions.

(2) Wear and failure surfaces have practically the same O/C ratio, wear surface 11.6%, failure surface 11.5%.

(3) Surfaces cleaned with water show much higher O/C ratio, i.e. failure surface 24.8%, wear surface 18.2%. This might be due to water molecules adsorbed on surface, or the removal of terrain which covered the sample surface.

(4) Increasing trend of O/C ratio with service mileage also prevails on Firestone pads filled with Kevlar fibers. The O/C ratio from 0 to 1000 miles are 1.6%, 3.3%, and 5.6%, sequentially.

ESCA analysis of cross-country pads shows, for pads with SBR rubber matrix, the O/C ratio at 250 miles is always higher than after 366 miles. The natural rubber matrix behaves just the opposite way and also performs superior to SBR pads in terms of wear resistance. Comparing results from the rubber matrix after swelling with toluene and drying, with the extracted residue from the swelling solution, ESCA spectra indicates much more oxygen in the remaining matrix. About the same amount of oxygen is in the solution residue of FS pad as appeared in the original spectra before extraction. The O/C ratio on the extracted pad surface was 3 to 5 times higher than in bulk as shown in Figure 4. This indicates that the O_2 incorporates primarily in the remaining insoluble network structure to increase the crosslink density, rather than in the capped short chains, which are the dried residue of the toluene solution used to extract low molecular weight moiety from the rubber pads. A concentration of oxygen decreases with increasing depth from the pad surface. A correlation between relative crosslink density and oxygen content of the FM pad surface was also observed. The increase of O_2 appears to increase the T_g and the extent of crosslinks in rubber matrix. Further examination of T_g and crosslinking on extracted pad surfaces will result in better understanding of the role of oxygen on changes in rubber properties.

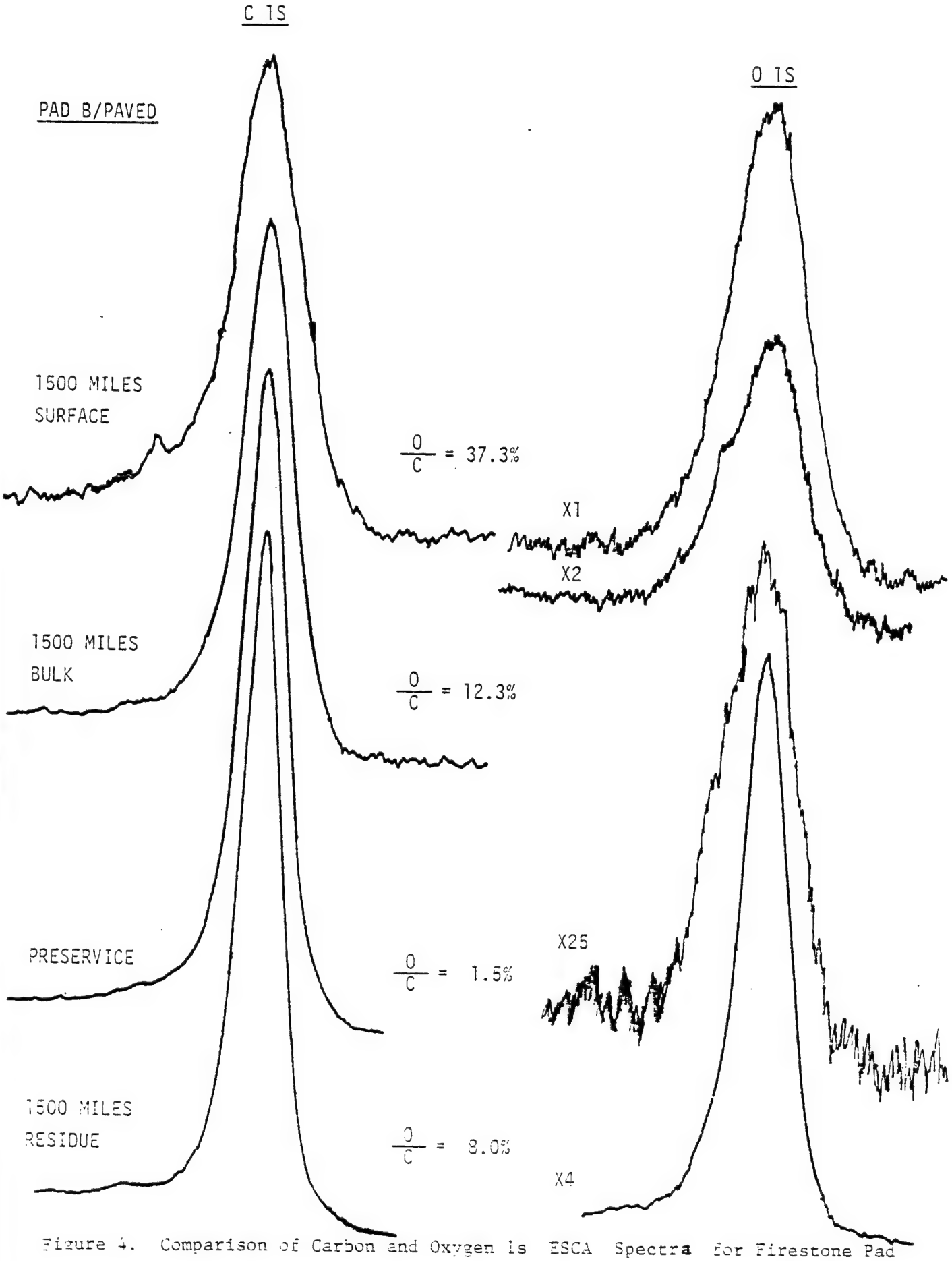

Figure 4. Comparison of Carbon and Oxygen 1s ESCA Spectra for Firestone Pad

4-7 Field Weight Loss

To make a more rational approach to the problem of track pad failure, we obtained statistical data on the mileage-to-failure for three courses from the YPG test program. The amount of rubber wear was measured on Standard Products, Goodyear and Firestone pads. Using the thickness between the bottom or wearing surface, and the flushing line or edge of the metal shoe as a measurement, we determined the percent abrasion of service pads with respect to the original pad thickness. Standard Products pads show better wear resistance than the other two manufacturers (Table G-1).

The study of T142 track pad weight loss data provided by TARADCOM reveals weight loss generally fall into two groups which may represent two different positions; namely the outside pad and inside pad on the track. This effect was most pronounced in the cross-country and least in paved service. By subtracting the shoe weight from the apparent weight in the data lists, the real weight loss of SBR elastomers is obtained and a performance comparison among track pads is then possible. For the paved course, abrasive wear is the principal mechanism and weight loss is more significant in the first and the last 500 miles. FM pads perform best, SP and GS second, and FT pads show the fastest weight loss. Consistently low performing, MK pads were second in wear rate.

For the gravel and the cross-country courses, the pad wear rate increases proportionally with mileage. The deviation from the paved course seems to be the result of a different meachnism. MK pads had the greatest weight loss, and FM pads the least.

T97E2 pads were designed to determine the geometric effect on the performance of track pad elastomer. Since they are of different metal shoe

size, the percentage loss of total weight does not reflect the actual comparison in severity of wear pads. The calculation of percent rubber loss indicates the performance of T97E2 pads is generally between the best T142 pad (FM pad) and the average T142 pads.

5. FUTURE RESEARCH

We plan to focus our future research efforts in three areas:

1. study of the failure mechanisms incurred by track pads in cross-country service during the full scale testing program at the Yuma Proving Grounds,
2. development of accelerated laboratory tests for (a) crack growth in notched tensile specimens under cyclic fatigue loading and (b) oxidation resistance via a DSC kinetics technique, and
3. development of new spectroscopic methods (NMR and FTIR) to characterize elastomer molecular structure.

The ESCA, SEM/EDXA, TMA, and solvent-swelling methods described earlier will be employed to identify submicroscopic, atomic-molecular, network and morphological structural aspects of cross-country pad failures. Samples will be selected from at least three manufacturers, and will include all the important generic types. Emphasis will be placed upon differences between sections (< 1mm thick) from surface, sub-surface and bulk. Standard procedure will include toluene extraction prior to analysis.

Concurrent development of two simulated laboratory tests of durability will probe:

1. crack growth under static and dynamic stress, and
2. time and temperature dependence of oxidation resistance.

Results to date clearly show that cutting and tearing mechanisms dominate in cross-country service. These mechanisms are modeled most simply by studies on the growth of a single, controlled crack or notch. Another certain conclusions is that the O/C ratio in the insoluble network increases with service. We expect that a rapid DSC test to rank antioxidant effectiveness will help predict track pad durability.

Our goal is an atomic-molecular model of the track pad failure process(es), and the relationship to the virgin pad composition. Therefore, we plan a significant effort to develop:

1. Fourier Transform Infrared and
2. C^{13} NMR Spectroscopic techniques,

and apply them to define the chemistry of pads, both as received and after service. A new magic angle spinning NMR is available now in the Chemistry Department. We are proposing a combination of funding be used to purchase the FTIR equipment.

REFERENCES

1. P. J. Flory, "Principles of Polymer Chemistry," Cornell Univer. Press, Ithaca and London, 1953.

2. S. Timoshenko, "Theory of Elasticity," McGraw-Hill, New York, 1934.

3. I. I. Vorvich and Iu. A. Ustinov, J. Appl. Math. Mech., 23, 637, (1959).

4. L. M. Kerr, Trans ASME, J. Appl. Mech., 143, (1964).

5. E. F. Finkin, Wear, 19, 277, (1972).

6. K. T. Gillen, Polymer Preprints, 17, 910, (1976).

7. L. R. G. Treloar, "Physics of Rubber Elasticity," 2nd ed., Oxford Univ. Press (Clarendon), London and New York, 1958.

8. J. Chiu, Applied Polym. Symposiu, 2 25-43 (1966).

9. J. J. Mauer, Rubber Chem and Tech., 42, 110, (1969).

10. D. W. Brazier and G. H. Nickel, Rubber Chem and Tech., 52, (4), 735 (1979).

11. A. N. Gent, Tran. Inst. Rubber Ind., 46, (1958).

12. D. W. Jopling and E. Pitts, J. Appl. Phys., 16, 541, (1975).

APPENDIX A

Swelling

Swelling

Although the computation of absolute crosslink density[1] was theoretically derived for crosslinked polymeric materials, the purpose of this swelling experiment is only to determine the relative crosslink density. Another reason for our limited goal is the well-known fact that the quantitative calculation of average molecular weight between crosslinks is not well resolved in filled elastomer vulcanizates. Furthermore, the absolute crosslink density is even meaningless since the loading level of carbon black in track pads is unknown to us. Therefore, the knowledge of relative crosslink density of same type pads will be useful enough on a comparative basis.

The procedure to carry out a swelling experiment by the gravimetric technique was given in the last Report, No. 12498, Contract # DAAK 30-78-C-0098. Additional attention is paid in the preparation of sample. For a preservice pad, the thickness of a sample is not critical. Yet for a service pad, the upper top layer may have different crosslink density than the underlayer; the wear portion may also be different from cracked sections. The preparation of a thin enough sample will certainly influence the outcome of % weight gain in swelling. The following equations were used to find out the relative crosslink density, 1/Q.

$$\% \text{ weight gain, } Q = 100 \times (W_S - W_O)/W_O$$

$$Q \propto 1/\#\text{ crosslink}$$

where W_S, the swollen sample weight; W_O, the original sample weight. The relative crosslink density is then defined as 1/Q.

Table A-1

SWELLING IN TOLUENE

Samples	% Gain in Weight	1/Q*
GK-0	159	0.629
GS-0	154	0.654
GS-P-500	153	0.654
GS-P-1000	150	0.667
GS-P-1500	152	0.658
FS-0	184	0.543
FS-P-500	155	0.645
FS-P-1000	186	0.538
FS-P-1500	187	0.535
SP-0	166	0.602
SP-P-500	166	0.602
SP-P-1000	166	0.602
SP-P-1500	165	0.606
FM-0	147	0.679
FM-P-500	145	0.692
FM-P-1000	133	0.757
FM-P-1500	123	0.811

Table A-2

RELATIVE CROSSLINK DENSITY OF PADS

Samples	Service Weight Loss (%)	250 Mile Cross Country		Preservice	
		% Gain in weight	1/Q*	% Gain in weight	1/Q*
GK-XC-250	41	146	0.684	159	0.628
GS-XC-250	57	147	0.678	154	0.649
FK-XC-250	23	164	0.609	---	---
FS-XC-250	41	140	0.714	184	0.543
SP-XC-250 SP#40**	51	143	0.700	166	0.603
SP-XC-250 SP#26	22	171	0.585	166	0.603

* Q=(swollen weight-original weight)/original weight

** SP#40 may be Monarch #40 since we can not find #40 in the list of Standard Product HSC 250

APPENDIX B

Compressive Modulus

Compressive Modulus

Generally speaking, the extent of penetration of a hard probe into a soft object is inversely related to the sample hardness. The modulus is in turn related to hardness in a more complicated manner. Nevertheless, an equation was derived for the interpenetration of elastic bodies.[2] The equation is limited to infinite sample height and time-independent quantities. In practice, once the time-dependent effect of Poisson ratios is neglected and the penetration depth is small, the correction to the equation is small.[3-5] Furthermore, by measuring the penetration distance at a fixed time period and neglecting a term containing the probe compliance (<1), a simplified equation[6] can be obtained to deal with viscoelastic materials as follows.

$$\frac{1}{D_S} = \frac{3/4(1-\nu_S^2)W}{R^{1/2}\, p^{3/2}}$$

where D_S, compliance of sample; ν_S, Poisson ratio of sample; R, radius of probe tip; W, weight on the probe; p, penetration depth.

The apparatus is a Perkin-Elemer Model TMS-2 schematically sketched in Figure B-1. The quartz probe which indents the sample is coupled to a weight tray through an LVDT core. The LVDT senses the penetration distance into the sample caused by the weight. Because of the float suspension, the weight tray requires a mass in the range of 2.1 to 2.8 gm in order to make the probe tip just touch the surface of the sample (zero-weight condition). Additional weight on the loading platform will cause indentation.

One basic probe of the Perkin-Elmer Model TMS-2 is the penetration probe, the tip of which is a small rod of known cross section (6.2×10^{-3} cm^2). For a given weight on the loading platform, the constant pressure can then be calculated. The TMA output shown on either a voltmeter or a chart recorder

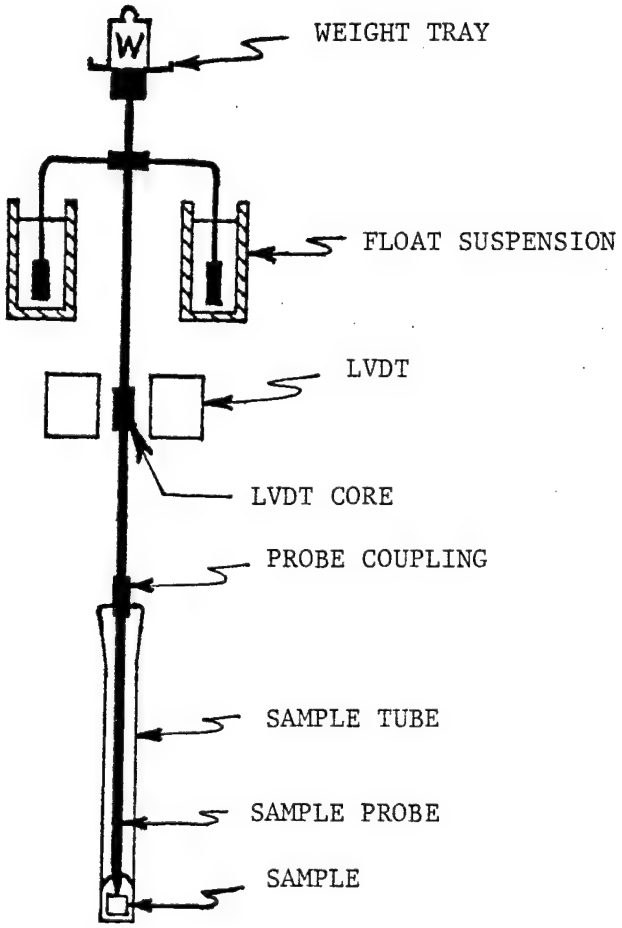

Figure B-1

Schematic Diagram of Perkin-Elmer TMS-2 Thermal Mechanical Analyzer

indicates the amount of penetration owing to the applied stress. Since the stress is maintained throughout the test, the time-dependent compressive creep of the sample is observed as loads are placed on or removed from the platform. Therefore, increasing stress added to the sample and the resultant strain measured on the TMS yield a compressive stress-strain curve for a fixed test time. For small loads the stress-strain relationship is linear and continuous at both the tensile and compressive regions[7] allowing the calculation of Young's Modulus from the slope. The modulus obtained is just relative since the probe tip is flat instead of the round tip used in the theoretical treatment.

APPENDIX C

Thermogravimetric Analysis (TGA)

TGA

Thermogravimetric Analysis (TGA) is a thermo-analytical technique in which the changes in weight of a material are followed as a function of temperature (dynamic TGA), or as a function of time at a specific temperature (isothermal TGA). Various applications of the thermogravimetry have been studied on relative thermal stability, analysis of additives, study of reaction kinetics, characterization of polymer blends and copolymer and others. Though the use of TGA in comparing thermal stability was generally recognized, the strict comparison of thermal stability can only be achieved by analyzing the samples of interest under indentical experimental conditions. However, different techniques involving variations in method and atmosphere of heating determined the influence of polymer structure and composition on thermal stability.[8] TGA analysis of a plasticizer in a high polymer system is usually tedious, if not hopeless. A rapid determination of the amount of plasticizer depends on whether the latter is completely volatilized prior to the polymer decomposition, and whether there is no reaction between the two. TGA was also utilized to study kinetics of processes, such as vaporazation, oxidative degradation.[8,9] Polyblend usually gives a thermogram consisting of separate weight loss regions corresponding to the components if their thermal stability are sufficiently different.

TGA study of the track pad elastomers was conducted with a Perkin-Elmer TGS-2 in couple with a System 4 microprocessor. The time-consumming calibration period was reduced to about 30 minutes with a built-in programmed calibration routine of the System 4. A piece of sample (@ 10 mg) was placed in a balance pan before the furnance tube with thermocouple was put into position around the sample pan. The system is purged with nitrogen and heated

at a rate of 20°C/min. The % weight loss vs. temperature is continuously recorded on the X-Y chart recorder.

Many factors important to TGA study were fixed by using a given commercial TGA unit. This leads to the consideration of sample size, heating rate, atmosphere, and temperature measurement as the major experimental variables. In study of vulcanized elastomers, if there is low level of volatile matter present, it may prefer to make an isothermal analysis, and to increase the sample size in order to yield a well-resolved thermogram.

J. J. Maurer[9] has developed a TGA procedure in his laboratory to determine the % polymer in vulcanizate by the calculation of % polymer remained in vulcanizate at specific temperature. The method has been effective to estimate oil content in butyl rubber vulcanizates through a correction curve for weight loss at T_R (400°C). The same reference temperature was employed in estimating the volatile content in various track pad elastomers.

APPENDIX D

Thermomechanical Analysis (TMA)

TMA

Theoretical treatments of modulus versus indentation for a round tip probe was mentioned in Compressive Modulus section in Appendix. The relationship is still applicable for the case of a flat tip probe if only the relative correlation between penetration and modulus is sought. From the indentation of a rigid sphere and BS 903, Gent[8] established a relation between Yount's modulus and Shore hardness. However, the measurement of hardness has very little meaning if the property changes of rubber take place only at very top thin layer. More thorough mathematical treatment was also derived[9] for a cylindrical plunger with radius much larger than sample thickness. Although the normal force is proportional to the depression and inversely proportional to the cube of the sample thickness, the absolute determination of modulus versus indentation is still not straight forward due to between probe and sample. In this derivation, the force versus displacement is different for the two cases just mentioned. Therefore, the moduli specified in this study are relative.

The schematic diagram in Figure B-1 indicates the part of the essential design feature of the analyzer. The penetration (indentation) probe makes contact with a sample. Temperature is exactly controlled by a linearized resistance thermometer. The low mass furnace is surrounded with an insulation tank filled with appropriate coolant. As the sample expands, contracts, or softens, the position of the probe will change and the change of position is accurately monitored by an LVDT (linear variable differential transformer). The electronic amplifier takes the output of the LVDT and converts it into a 10 millivolt signal to the recorder. The instrument is also provided with a switch to allow selection of either the English (range from 0.002 to 0.1 inch)

or the metric (range from 0.05 to 2.5 millimeters) scale. The control unit also provides an amplified signal to a first derivative computer (FDC) module so that the rate of the probe displacement may be simultaneously precorded with the probe position on the two pen x-y or strip chart recorder. TMS-2 shares the same heater control unit with TGS-2 for TGA study and also the same System 4 microprocessor for temperature calibration and temperature control program.

A "modulus" versus temperature TMA and DTMA thermogram is shown in Figure D-1. Lists of TMA data are also shown in Tables D-8 to D-13.

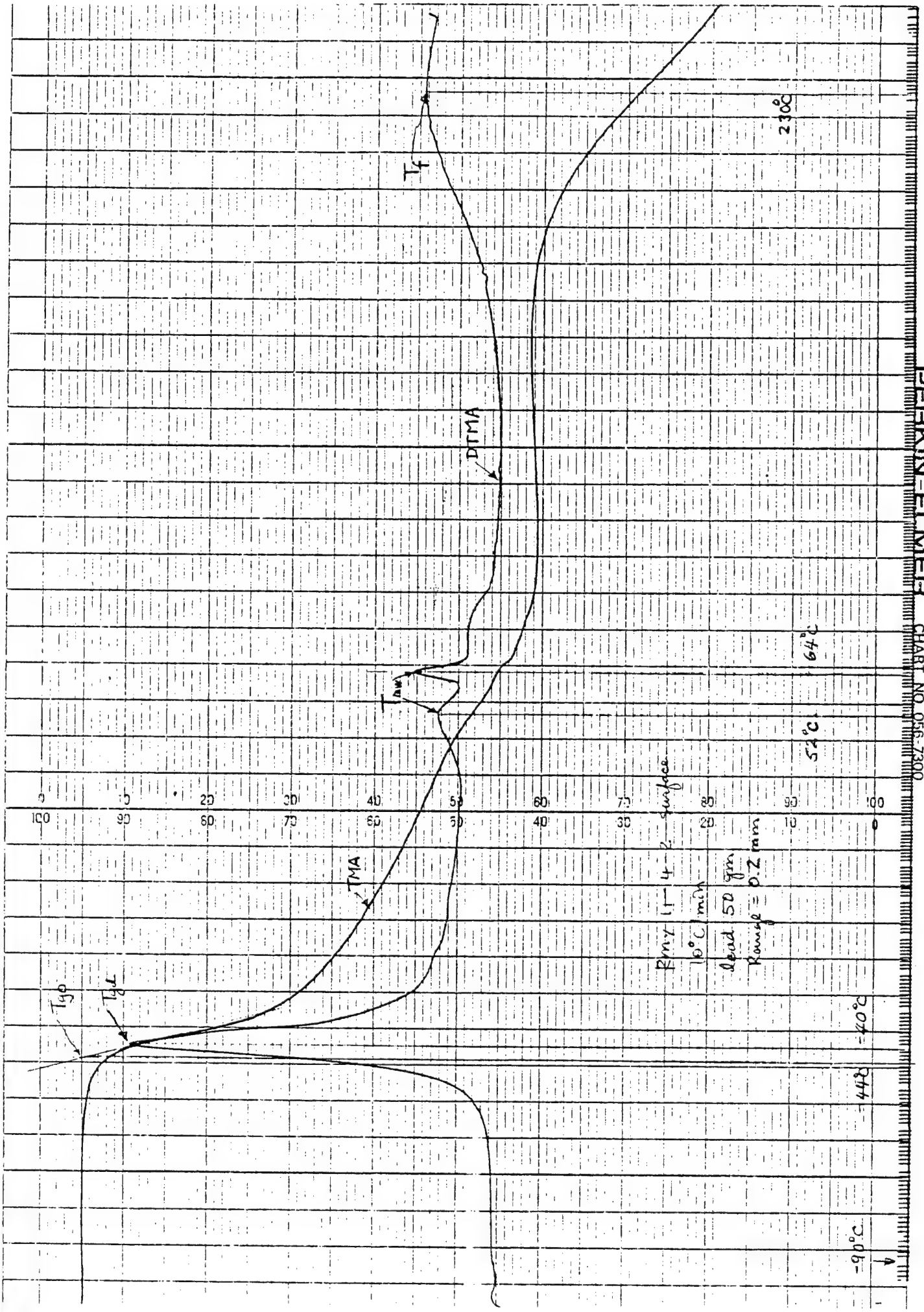
PERKIN-ELMER
CHART NO. 056-7300
T_f
DTMA
TMA
T_{DW}
T_{yp}
T_{yL}
2300
64°C
54°C
-40°C
-90°C
Lead 50 gm
Ramp = 0.2 mm
10°C/min
Env. 1 — 4 — 2 surface

Figure D-1

TABLE D-1

TGA Data of Goodyear Kevlar Fibre Filled SBR (GK) Pads

Sample	Sample Weight (mg)	1st DTGA Peak (°C)	2nd DTGA Peak (°C)	Major DTGA Peak (°C)	Temperature of 10% Loss (°C)	% Loss at 400°C	Selected Region
0	9.83	340	427 & 441	498	366	12.7%	surface
P-500	9.68	341	-	501	360	13.4%	"
P-1500	9.57	344	-	506	367	13.6%	"
XC-250	9.59	347	-	493	352	14.8%	wear
XC-250	9.47	336	-	502	371	11.8%	crack
XC-366	9.59	337	-	509	347	15.0%	wear
XC-366	9.63	345	-	504	364	12.8%	crack
G-1000	9.64	-	-	507	367	15.2%	wear
G-1000	9.68	337	-	494	390	11.4%	crack

DTGA: differential TGA

Heating Rate = 20°C/min

Atmosphere = N_2

TABLE D-2

TGA Data of Goodyear SBR (GS) Pads

Sample	Sample Weight (mg)	1st DTGA Peak (°C)	2nd DTGA Peak (°C)	Major DTGA Peak (°C)	Temperature of 10% Loss (°C)	% Loss at 400°C	Selected Region
0	7.32	332	-	502	336	15.8%	surface
P-500	7.65	335	-	492	341	15.5%	"
P-1500	7.35	332	-	489	341	15.4%	"
XC-250	7.62	337	-	486	345	15.6%	wear
XC-250	7.48	323	-	470	349	14.8%	crack
XC-366	7.63	324	-	481	339	16.8%	wear
XC-366	7.38	331	-	481	353	16.2%	crack

DTGA: differential TGA

Heat Rate = 20°C/min

Atmosphere = N_2

TABLE D-3

TGA Data of Firestone Kevlar Fibre Filled SBR (FK) Pads

Sample	Sample Weight (mg)	1st DTGA Peak (°C)	2nd DTGA Peak (°C)	Major DTGA Peak (°C)	Temperature of 10% Loss (°C)	% Loss at 400°C	Selected Region
0	9.71	-	433	492	387	11.3%	surface
P-500	10.1	-	441	495	384	11.5%	"
P-1500	9.99	323	-	489	376	11.9%	"
XC-250	9.98	325	-	483	377	12.7%	wear
XC-250	9.65	-	-	470	375	12.6%	crack
XC-366	9.82	-	-	482	374	12.5%	wear
XC-366	8.84	-	-	481	382	12.0%	crack
G-1000	9.81	-	-	477	381	12.8%	wear
G-1000	10.1	-	-	479	396	10.5%	crack

DTGA: differential TGA

Heat Rate = 20°C/min

Atmosphere = N_2

TABLE D-4

TGA Data of Firestone SBR (FS) Pads

Sample	Sample Weight (mg)	1st DTGA Peak (°C)	2nd DTGA Peak (°C)	Major DTGA Peak (°C)	Temperature of 10% Loss (°C)	% Loss at 400°C	Selected Region
0	8.19	-	-	484	379	12.2%	surface
P-500	7.65	315	-	489	372	12.1%	"
P-1500	7.69	-	453	493	383	11.7%	"
XC-250	7.61	-	439	491	385	11.4%	wear
XC-250	7.52	-	-	480	381	12.2%	crack
XC-366	7.72	-	-	490	384	11.4%	wear
XC-366	7.53	-	-	499	388	11.4%	crack
G-1000	7.59	306	-	497	377	12.1%	wear
G-1000	7.61	-	-	489	395	10.8%	crack

DTGA: differential TGA

Heating Rate = 20°C/min

Atmosphere = N_2

TABLE D-5

TGA Data of Standard Product SBR (SP) Pads

Sample	Sample Weight (mg)	1st DTGA Peak (°C)	2nd DTGA Peak (°C)	Major DTGA Peak (°C)	Temperature of 10% Loss (°C)	% Loss at 400°C	Selected Region
0	7.32	336	424	481	379	12.4%	surface
P-500	6.96	325	-	507	355	13.5%	"
P-1500	7.25	337	440	482	361	12.8%	"
XC-250	7.00	318	-	481	349	15.6%	wear
XC-250	7.01	317	-	480	358	14.1%	crack
XC-366	7.01	323	-	481	367	14.5%	wear
XC-366	7.08	323	-	478	364	14.4%	crack

DTGA: differential TGA

Heat Rate = 20°C/min

Atmosphere = N_2

TABLE D-6

TGA Data of Firestone Experimental SBR (FM) Pads

Sample	Sample Weight (mg)	1st DTGA Peak (°C)	2nd DTGA Peak (°C)	Major DTGA Peak (°C)	Temperature of 10% Loss (°C)	% Loss at 400°C	Selected Region
0	8.14	338	428	481	356	14.2%	surface
P-500	8.07	321	448	483	352	14.6%	"
P-1500	7.78	326	-	478	347	15.1%	"
XC-250	7.81	320	-	475	355	13.6%	wear
XC-250	7.98	324	-	482	361	13.4%	crack
XC-366	8.02	323	-	500	387	12.1%	wear
XC-366	8.05	334	-	486	393	11.2%	crack
G-1000	8.05	327	-	490	344	12.9%	wear
G-1000	8.17	-	-	485	395	10.5%	crack

DTGA: differential TGA

Heating Rate = 20°C/min

Atmosphere = N_2

TABLE D-7

TGA Data of Firestone Triblend (FT) Pads

Sample	Sample Weight (mg)	1st DTGA Peak (°C)	2nd DTGA Peak (°C)	Major DTGA Peak (°C)	Temperature of 10% Loss (°C)	% Loss at 400°C	Selected Region
0	9.13	-	419	479	364	16.7%	surface
XC-250	9.00	-	-	421 & 431	352	19.7%	wear
XC-250	9.18	-	-	413	360	23.2%	crack
XC-366	9.10	-	-	484	425	7.8% (?)	"
XC-366	9.02	-	-	417	360	20.6%	wear

DTGA: differential TGA

Heat Rate = 20°C/min

Atmosphere = N_2

Table D-8

Glass Transition Temperature of Cross-Country Pads

Sample		load (gm)	T_{gd}* (°C)
GK-XC-250	Crack	20	-36
	"	20	-37
	"	20	-35
	"	40	-36
	Wear	50	-31
GS-XC-250	Wear	50	-34
	Crack	50	-32
FK-XC-250	Wear	50	-40
	Crack	50	-30
FS-XC-250	Wear	50	-37
	Crack	50	-31
SP-XC-250	Wear	50	-38
	Crack	50	-36

*T_g taken at the peak of derivative TMA curve.
Heating rate: 10°C/min.

Table D-9

TMA, TGA Thermal Data of Track Pads on Paved Course

Sample	Service Life (miles)	T_{vf}* (°C)	T_g** (°C)	% Weight loss at 400°C
A***	0	215	-40	15.8
	500	213	-38	15.5
	1500	213	-37	15.4
B***	0	230	-40	12.2
	500	216	-37	12.1
	1500	214	-36	11.7
C***	0	226	-38	12.4
	500	219	-43	13.5
	1500	218	-40	12.8

* T_{vf} : viscous flow temperature defined as the temperature where the maximum change of hardness in the terminal zone takes place.

** T_g : glass transition temperature

*** A:GS; B:FS; C:SP

Table D-10

TMA, TGA Thermal Data of Track Pads on Cross Country Course

Sample	Service Life (miles)	T_{vf}* (°C)	T_g** (°C)	% Weight Loss at 400°C
A***	0	215	-40	15.8
	250	218	-34	15.6
	366	205	-37	16.8
B***	0	230	-40	12.2
	250	215	-37	11.4
	366	220	-36	11.4
C***	0	226	-38	12.4
	250	219	-38	15.6
	366	210	-34	14.5

* T_{vf} : viscous flow temperature defined as the temperature where the maximum change of hardness in the terminal zone takes place.

** T_g : glass transition temperature

*** A:GS; B:FS; C:SP

. CORRELATION BETWEEN T_g AND TGA % WEIGHT L SS AT 400°C. GREATER VOLATILE CONTENT WILL LEAD TO MORE CHAIN MOBILITY, THUS LOWER T , IF OTHER MOLECULAR PARAMETERS REMAIN THE SAME. ONLY PAVED COURSE SHOWED A CONSIST T TREND, INDICATING THAT TERRAIN MAY DOMINATE OVER MOLECULAR NETWORK FACTORS ! THE OTHER CASES.

Table D-11

TMA Data of Track Pad Elastomers

Samples	Load (gms)	T_{gx} (a) (°C)	T_{gd} (b) (°C)	T_{vf} (c) (°C)	T Span* (d) (°C)	Selected Regions
GS-0	50	-42	-38	216	254	surface
	50	-44	-39	-	-	bulk
	50	-45	-41	-	-	bulk
GS-P-500	50	-44	-38	212	250	wear
	50	-46	-38	213	251	wear
GS-P-1500	50	-40	-36	213	249	wear
	50	-43	-38	214	252	wear
GS-XC-250	50	-36	-32	-	-	crack surface
	50	-39	-34	218	252	wear surface
GS-XC-366	50	-42	-37	217	254	crack surface
	50	-43	-37	205	242	wear surface
GK-0	50	-42	-38	215	253	surface
	50	-44	-40	216	256	bulk
GK-P-500	50	-41	-36	-	-	wear
	50	-46	-39	213	252	wear
GK-P-1500	50	-45	-40	213	253	wear
	50	-45	-40	212	252	wear
GK-XC-250	20	-39	-36	-	-	crack surface
	20	-40	-37	-	-	crack surface
	20	-40	-35	213	248	crack surface
	40	-40	-36	216	252	crack surface
	50	-37	-31	217	248	wear surface
GK-XC-366	50	-45	-39	213	252	crack surface
GK-G-1000	50	-47	-39	210	249	crack surface

Table D-12

TMA Data of Track Pad Elastomers

Samples	Load (gms)	T_{gx} (a) (°C)	T_{gd} (b) (°C)	T_{vf} (c) (°C)	T Span* (d) (°C)	Selected Regions
FK-0	50	-44	-40	230	270	surface
	50	-43	-38	232	270	bulk
	50	-43	-37	227	264	bulk
FK-P-500	50	-42	-36	218	254	wear
	50	-44	-39	226	265	bulk
FK-P-1500	50	-41	-37	212	249	wear
	50	-43	-38	214	252	wear
	50	-45	-41,-37	210	251,247	wear
FK-XC-250	50	-35	-30	219	249	crack surface
	50	-44	-40	211	251	wear surface
FK-XC-366	50	-44	-39	216	255	crack surface
FK-G-1000	50	-42	-35	214	249	crack surface
	50	-42	-38	-	-	crack surface
FS-0	50	-44	-40	230	270	surface
	50	-47	-41	229	270	bulk
FS-P-500	50	-43	-36	215	251	wear
	50	-43	-38	217	255	wear
FS-P-1500	50	-40	-37,-34	-	-	wear
	50	-43	-35	230	265	wear
	50	-44	-36	221	257	wear
FS-XC-250	50	-35	-31	226	257	crack surface
	50	-41	-37	215	252	wear surface
FS-XC-366	50	-46,-43	-40,-34	-	-	crack surface
	50	-42	-38	-	-	crack surface
	50	-42	-35	218	253	crack surface
	50	-40	-31	-	-	wear surface
	50	-41	-36	220	256	wear surface

Table D-13

TMA Data of Track Pad Elastomers

Samples	Load (gms)	T_{gx} (a) (°C)	T_{gd} (b) (°C)	T_{vf} (c) (°C)	T Span* (d) (°C)	Selected Regions
SP-0	50	-44	-39	-	-	surface
	50	-42	-37	227.5	264.5	surface
	50	-42	-39	225	264	surface
	50	-41	-38	226	264	bulk
SP-P-500	50	-46	-43,-38	219	262,257	wear
	50	-47	-43	-	-	wear
SP-P-1500	50	-45	-40	219	259	wear
	50	-46	-40	217	259	wear
	50	-45	-40	221	261	wear
	50	-43	-40	222	262	wear
SP-XC-250	50	-40	-36	226	262	crack surface
	50	-43	-38	219	257	wear surface
SP-XC-366**	50	-47	-35	212	247	crack surface
	50	-43	-35	210	245	wear surface
	20	-46	-35	-	-	wear surface
	40	-43	-33	-	-	wear surface
FM-XC-250	50	-38	-34	210	244	crack surface
	50	-44	-38	215	253	crack surface
FM-XC-366	50	-46	-37	214	251	
FT-XC-250	50	-54	-50	185	235	crack surface*
FT-XC-366	50	-44	-38	215	253	crack surface
FA-XC-250	50	-46	-41	198	239	crack surface*
FA-XC-250	50	-45	-40	-	-	crack surface*
FA-XC-250	50	-71,-69	-57,-49	197	254,246	crack surface
FA-XC-366	50	-56	-51	209	260	crack surface
FA-G-1000	50	-70,-69	-62,-49	201	250	crack surface
MK-G-1000	50	-47	-40	204	244	crack surface
T97E2-G-1000	50	-43	-38	210	248	wear surface

(a) T_{gx} = softening temperature of polymer in the glassy zone obtained by the extrapolation of "modulus" versus temperature curve in glassy and transition zones.

(b) T_{gd} = glass transition temperature obtained from the temperature where the peak of differntial modulus vs. temperature curve locates.

(c) T_{vf} = viscous flow temperature defined as the temperature where the maximum change of hargness takes place in the terminal zone.

(d) T span = T_{vf}-T_{gd}

APPENDIX E

Electron Spectroscopy for Chemical Analysis

(ESCA)

ESCA

The ESCA instrument employed is a DuPont 650 X-ray photoelectron spectrometer with a magnesium anode. The general background theory on the electron spectroscopy was briefly mentioned in the last Report. It is well known that ESCA (Electron Spectroscopy for Chemical Analysis) is one of the most ideally suited techniques to investigate the chemical nature of surfaces.

As an X-ray beam of energy $h\nu$ shines on the material, photoelectrons are ejected from individual atoms interacted with the incoming photons. After sorting the kinetic energy of electrons and focusing on a detector, the detector produces an electrical signal proportional to the intensity of the emitted photoelectron. The readout system produces signals vs their binding energy, $E_b(e^-) = H\nu\text{-}KE$.

Moreover, chemical bonding or oxidation states will change the chemical environment of an atom in a molecule and so produce chemical shifts in binding energy. These shifts can be used to follow the chemical reaction that takes place on a polymer surface.

The oxidative degradation of track pad is clearly the most interesting topic in this study. The O/C ratio vs the service mileage was studied and shown in Figures E-1 and E-2. Figure E-1 shows the O/C ratio changes in pavement service, while Figure E-2 shows the cross-country course. The correlation among O/C ration, T_g and volatile content is indicated in Figure 3. The detailed ESCA composition information on most of the track pads is listed from Table E-1 to E-6.

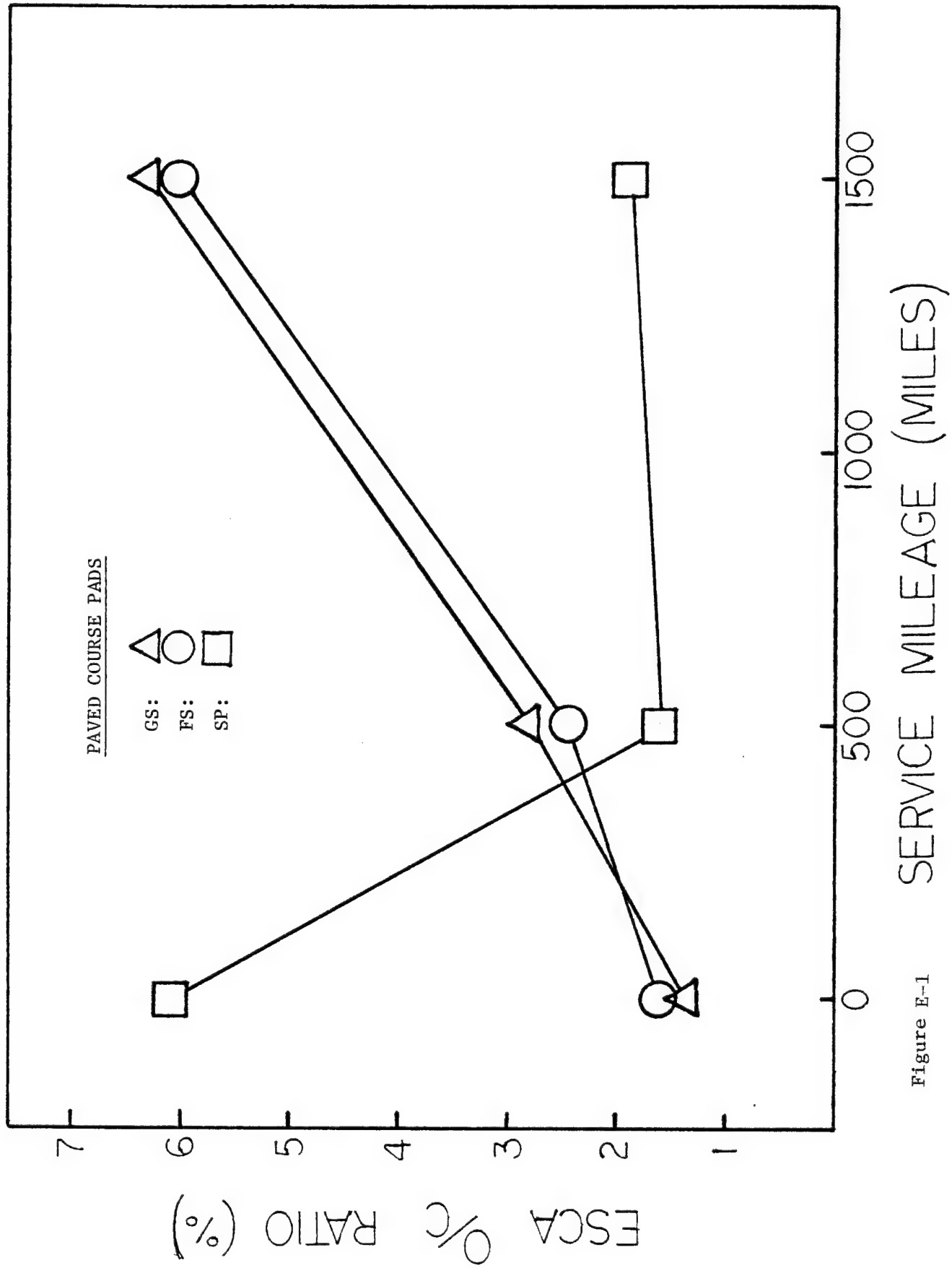
ESCA O/C RATIO (%)
7
6
5
4
3
2
1
0
500
1000
1500
SERVICE MILEAGE (MILES)
PAVED COURSE PADS
GS:
FS:
SP:

Figure E-1

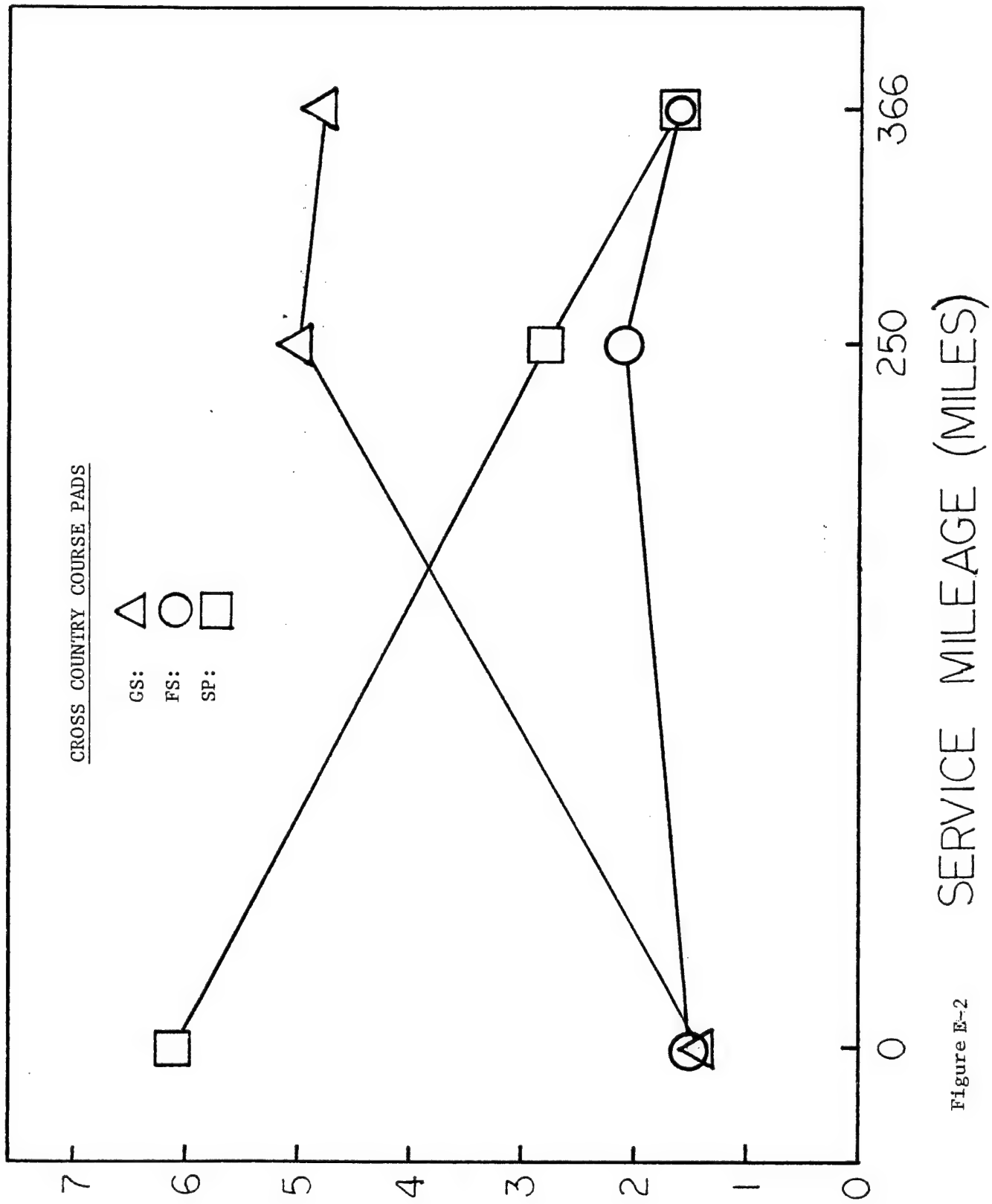
CROSS COUNTRY COURSE PADS
GS:
FS:
SP:
ESCA % RATIO (%)
SERVICE MILEAGE (MILES)
0
1
2
3
4
5
6
7
0
250
366

Figure E-2

Table E-1

ESCA Peak Assignments and Concentrations in Atom Percent of Goodyear Kevlar Fiber Filled (GK) Pads

Sample		C	O	N	Si	S	Zn	O/C (%)
GK-0	surface	84.6	7.3	1.7	7.5	0.5	-	8.63
		88.2	6.4	1.0	4.5	-	-	7.26
		94.1	3.3	0.9	1.3	0.2	-	3.51
	bulk	88.6	5.8	-	5.2	0.7	0.05	6.57
		88.3	5.6	-	5.4	0.5	0.1	6.34
GK-P-500		91.1	4.8	0.8	-	1.1	2.1	5.27
GK-P-1500		92.4	6.9	-	-	-	0.7	7.47
		93.2	5.9	-	-	-	0.9	6.33
GK-XC-250		91.3	5.9	1.6	0.8	-	0.6	6.46
GK-XC-366		93.8	3.9	1.2	-	0.6	0.5	4.16

Table E-2

ESCA Peak Assignments and Concentrations in Atom Percent of Goodyear SBR (GS) Pads

Sample		C	O	N	Si	S	Zn	O/C (%)
GS-0	surface	92.5	3.3	1.1	2.9	0.29	0.1	3.56
	bulk	97.1	1.4	0.9	0.5	0.1	-	1.44
GS-P-500		96.5	2.7	-	0.4	0.3	-	2.80
GS-P-1500		92.5	5.8	1.1	-	-	0.7	6.27
Wear Surface/H_2O		79.2	14.4	1.5	4.6	-	0.4	18.23
Fracture Surface/H_2O		72.5	18.0	2.4	5.9	-	1.0	24.83
Inside Fracture		90.5	5.7	1.3	0.8	0.6	1.1	6.30
Outside Fracture		83.4	9.6	2.0	4.8	-	0.2	11.51
		87.8	10.2	0.7	-	0.6	0.8	11.61
GS-XC-250		92.7	4.6	1.4	-	0.6	0.7	5.0
GS-XC-366		92.2	4.4	1.1	1.1	0.6	0.7	4.8

Table E-3

ESCA Peak Assignments and Concentrations
in Atom Percent of FK Pads

Sample		C	O	N	Si	S	Zn	O/C (%)
FK-0	surface	91.3	3.5	1.3	1.1	-	-	3.83
		98.2	0.6	0.4	-	-	0.8	0.61
	bulk	97.2	1.5	0.7	0.5	-	-	1.54
		97.7	1.4	0.9	-	-	-	1.43
FK-P-500		95.7	3.2	0.2	0.7	-	0.2	3.34
FK-P-1000		93.1	5.2	1.0	-	-	0.8	5.59
FK-XC-250		94.5	2.0	0.9	2.1	-	0.6	2.1
FK-XC-366		97.1	2.0	0.8	-	-	0.2	2.1

Table E-4

ESCA Peak Assignments and Concentrations
in Atom Percent of FS Pads

Sample		C	O	N	Si	S	Zn	O/C (%)
FS-0	surface	98.2	0.7	0.1	0.3	-	-	0.71
	bulk	97.3	1.5	0.3	0.4	-	-	1.54
FS-P-500		96.4	2.4	0.5	-	0.5	0.2	2.49
FS-P-1500		94.6	4.2	1.0	-	-	0.4	4.44
FS-P-1500	extracted surface	6.59	24.6	3.1	3.7	-	1.8	37.7
	extracted bulk	90.3	8.1	0.9	-	0.7	-	9.0
		86.0	10.6	0.5	2.2	0.5	0.2	12.3
	solution residue	90.9	7.1	1.1	-	0.7	-	8.0
FS-XC-250		96.7	2.0	0.5	0.7	-	0.1	2.1
FS-XC-366		98.2	1.6	-	-	-	0.2	1.6

Table E-5

ESCA Peak Assignments and Concentrations
in Atom Percent of SP Pads

Sample		C	O	N	Si	S	Zn	O/C (%)
SP-0	surface	95.7	0.5	0.3	-	-	-	0.52
		98.8	0.7	0.2	0.3	-	-	0.71
	bulk	88.6	6.0	0.7	0.8	0.6	0.9	6.77
		92.1	5.0	0.8	1.5	0.5	-	5.43
SP-0 Surface/Razor Blade		96.0	2.3	0.6	0.6	0.3	0.2	2.4
SP-P-500		98.5	1.5	-	-	-	-	1.52
SP-P-1500		98.1	1.4	0.4	-	-	0.2	1.43
		98.0	2.2	0.7	-	-	0.1	2.27
SP-P-1500	extracted surface	65.2	31.1	2.7	-	1.1	-	47.7
	solution residue	90.5	7.6	1.3	-	0.5	-	8.4
SP-XC-250		96.5	2.5	0.6	-	-	0.4	2.6
SP-XC-366		98.2	1.6	-	-	-	0.1	1.6

Table E-6

ESCA Peak Assignments and Concentrations in Atom Percent of MK, FT, FM and FA Pads

Sample		C	O	N	Si	S	Mg	O/C (%)
MK-O	surface	96.2	1.9	0.6	0.7	0.5	-	1.98
		97.8	1.4	0.2	0.4	0.2	-	1.43
	bulk	97.6	1.0	1.0	0.3	0.1	-	1.02
		98.2	0.9	0.4	0.5	-	-	0.92
FT-O	surface	89.5	4.7	0.6	1.9	-	3.7	5.25
		95.6	2.2	1.1	0.8	0.2	-	2.3
	bulk	92.8	2.5	0.9	1.2	-	2.6	2.69
		98.0	0.7	0.8	0.3	0.2	-	0.71
FT-XC-250		83.6	1.24	0.7	2.4	0.4	-	14.8
FT-XC-366		86.5	8.8	1.3	1.9	1.0	-	10.2

Sample		C	O	N	Si	S	Mg	Zn	O/C (%)
FM-O	surface	98.6	0.4	0.2	0.2	-	0.6	-	0.41
	bulk	97.7	1.1	0.2	0.3	-	0.7	-	1.13
FM-P-500		95.2	3.5	-	0.8	0.5	-	-	3.68
FM-XC-250		99.1	0.9	-	-	-	-	-	0.91
FM-XC-366		91.1	5.6	1.2	0.9	0.7	-	0.5	6.1
FA-XC-250		95.5	3.4	0.7	-	0.3	0	0.1	3.6
FA-XC-366		92.3	6.3	0.9	-	0.3	-	0.2	6.8

APPENDIX F

Scanning Electron Microscopy/Energy Dispersive X-Ray Analysis (SEM/EDXA)

SEM/EDXA

The general principle of scanning electron microscope (SEM) was also illustrated in the last Report, No. 12498, Contract # DAAK 30-78-C-0098. As a result of bombardment on the specimen with high energy electrons, emitted are primary electrons, secondary electrons and X-ray. Primary electrons (or backscattered electrons) usually are of high energy and not collected by the detector. A dector (photomultiple tube with phospher screen and 15 KV accelerating power) collected secondary electrons and showed the image of local morphology. In coupling of scanning circuit to the scanning coils both in the electron optical column and in the cathode ray tube (CRT), electron beam can scan across certain region of a sample to access the overall surface morphology. The characteristics of emitted X-ray will be served to analyze the chemical composition in the bombardment region (EDXA).

The fractography of track pads on different test courses was studied. Samples studied were selected from wear surfaces, crack surfaces, and bulks beneath wear and crack portion. The interesting features in fractographs, e.g., particles, fibres, brittle fracture regions, were investigated further with the aid of EDXA chemical point analysis. In one case, SEM micrographs of crack initiation site show brittle fracture in which EDXA found high level of sulfur. Generally, the uncleaned surfaces are similar to one another microscopically. Variation in the sample preparation, such as surfaces cleaned or soaked with solvent, bulk samples cut normal or parallel to surface, given some distinguishable and meaningful features in the fractography (Figures F-1 to F-6).

Figure 9 A. Rapid degraded adhesive texture found at the interface of track pad metal shoe and rubber.

B. Clumps of zinc oxide particles were common fracture initiation sites.

C. A brittle region was found at the beginning of the crack leading to "chunk" failure in the paved course pad.

D. EDXA spectrum shows the brittle fracture region consists of a high level of sulfur, and therefore likely to be highly crosslinked.

Figure 10 A. General feature of a preservice pad surface.

B. Bulk morphology of a preservice Kevlar fiber filled SBR pad, with fiber length of about 1 mm.

C. Another feature of bulk morphology.

D. EDXA spectrum shows the surface contains nothing but rubber vulcanizate itself.

Figure 11 A and B. General appearance of fracture surfaces. Note debris of small particles of rubber and terrain. EDXA shows that the surface is dominated by terrain particles. Note the weak signal of rubber.

C and D. Uncleansed surface is heavily contaminated with terrain particles. No signal of rubber shown in EDXA spectrum.

Figure 12 A and B. Surfaces cleaned with toluene show granulated morphology

C and D. After extracted with toluene, the remaining matrix shows more granulated and porous morphology.

Figure 13 A and B. Different brightness regions were usually observed in the bulk cut normal to wear surface.

C. Swollen bulk of wear section generally shows no particular feature in the background morphology.

D. Some swollen bulk of wear section shows void and porous morphology.

Figure 14 A and B. Bulk morphology just beneath the wear surface generally shows pitches of different brightness.

C and D. Bulk morphology just beneath the crack surface shows pitches of different brightness occasionally. Particles D are Kevlar fibers and zinc oxide. Dark circles around ZnO particles may indicate different composition density.

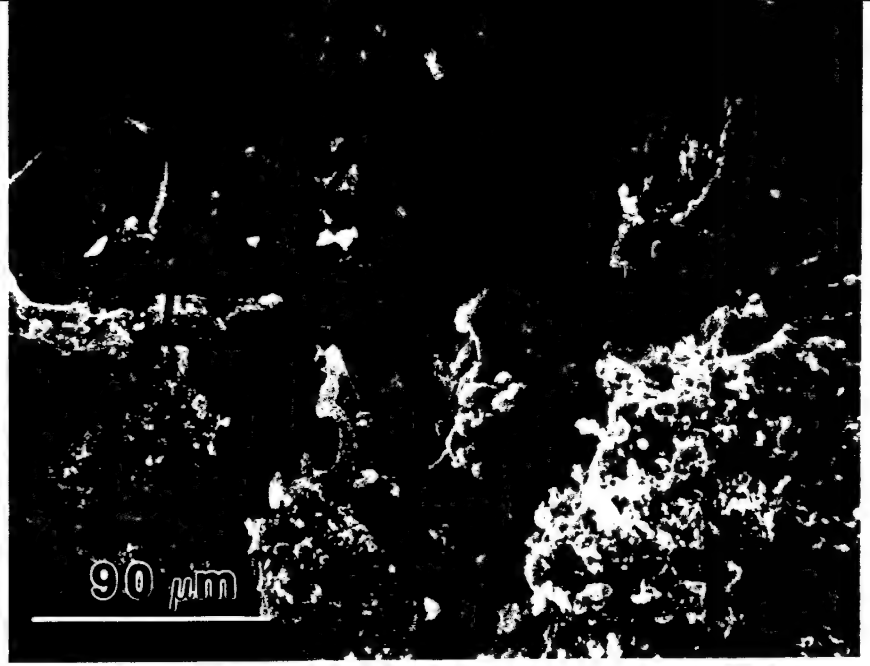

A

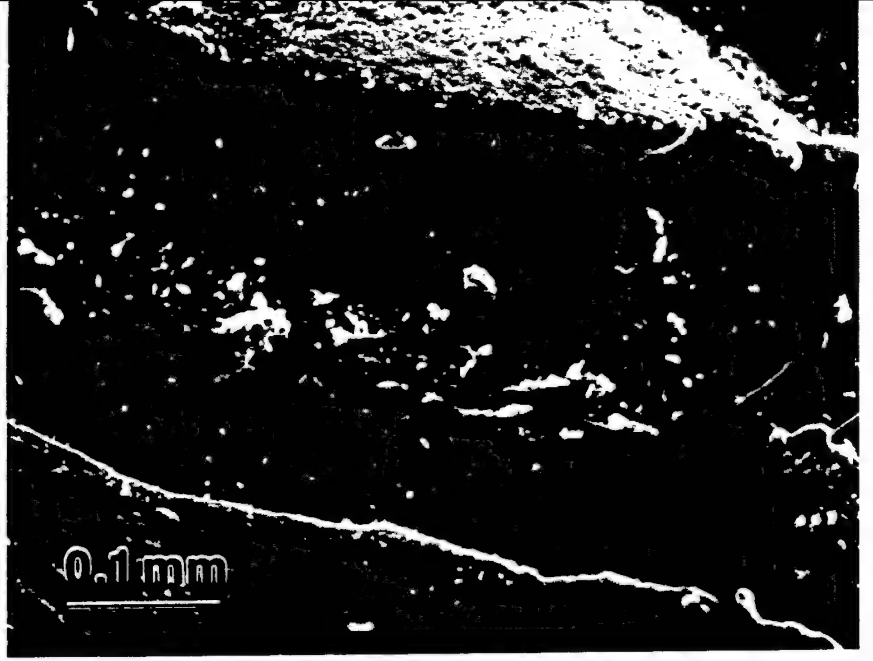

C

B

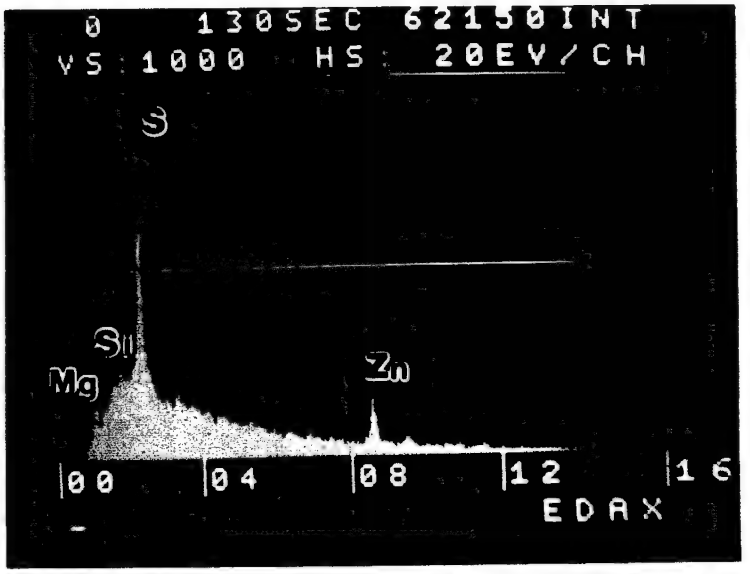

D

Figure F-1

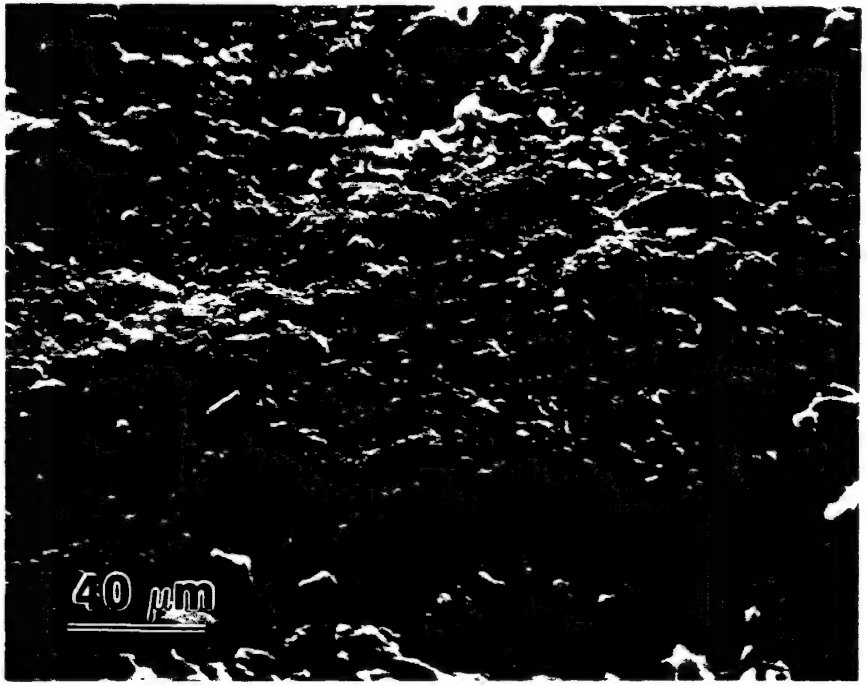

A

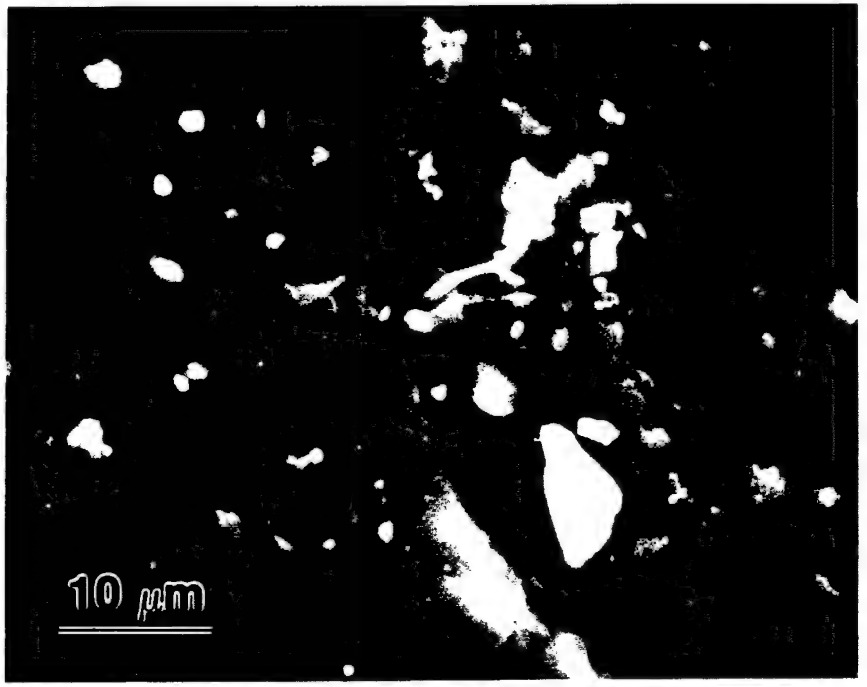

C

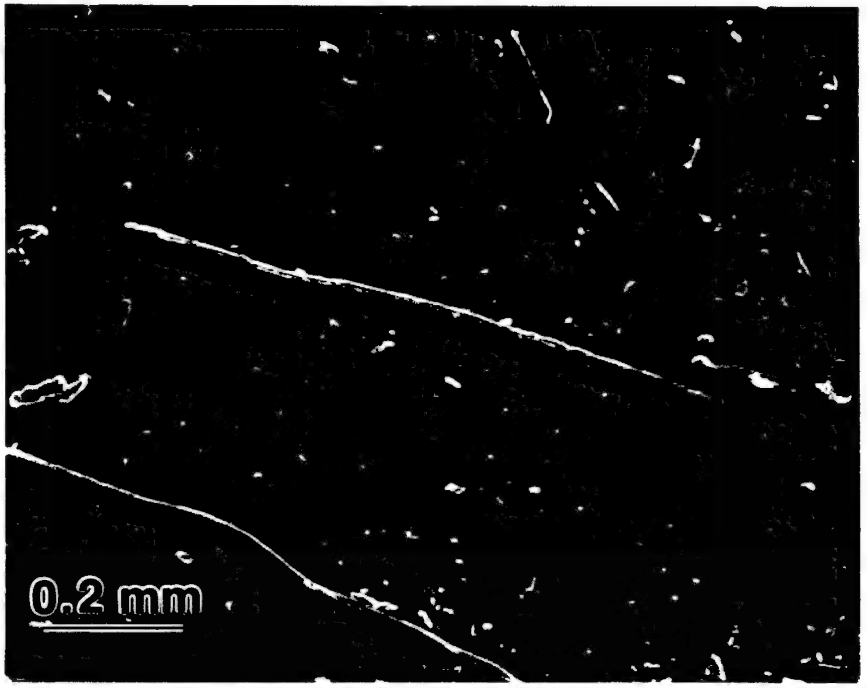

B

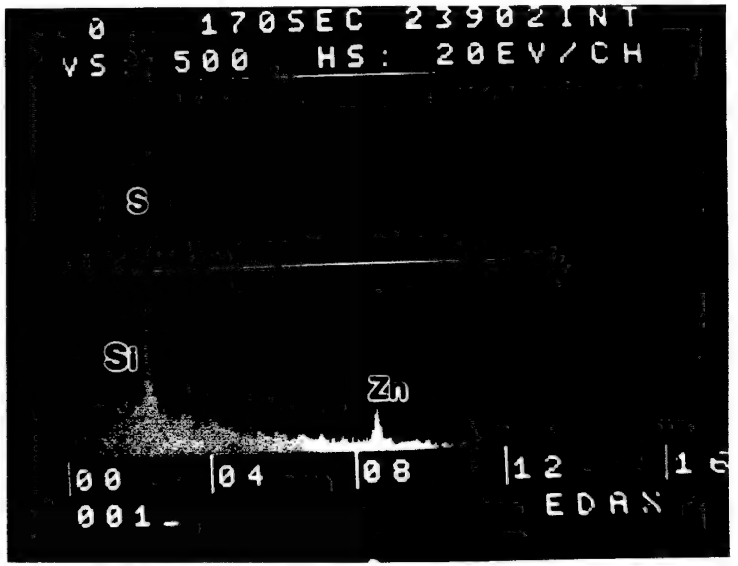

D

Figure F-2

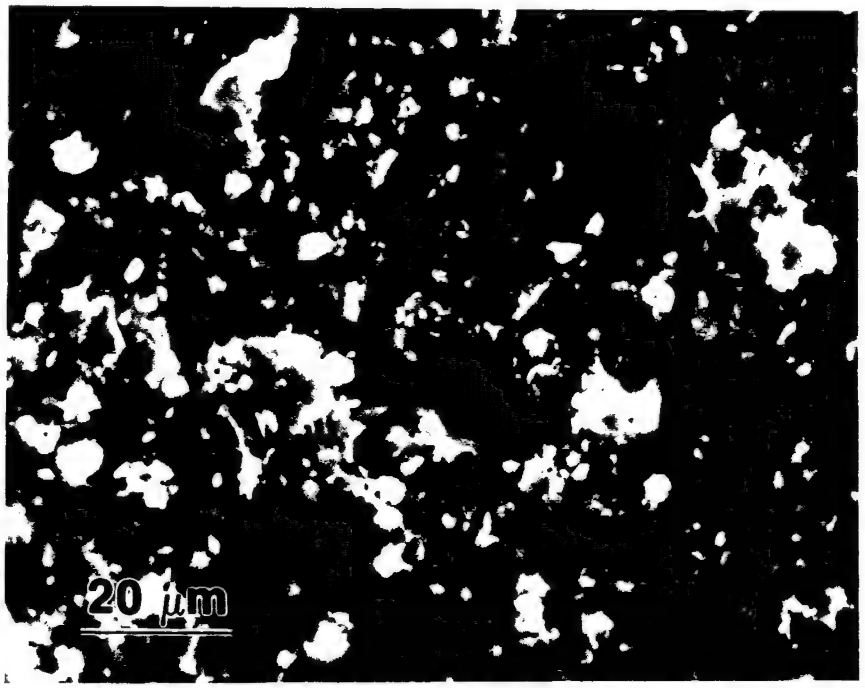

A

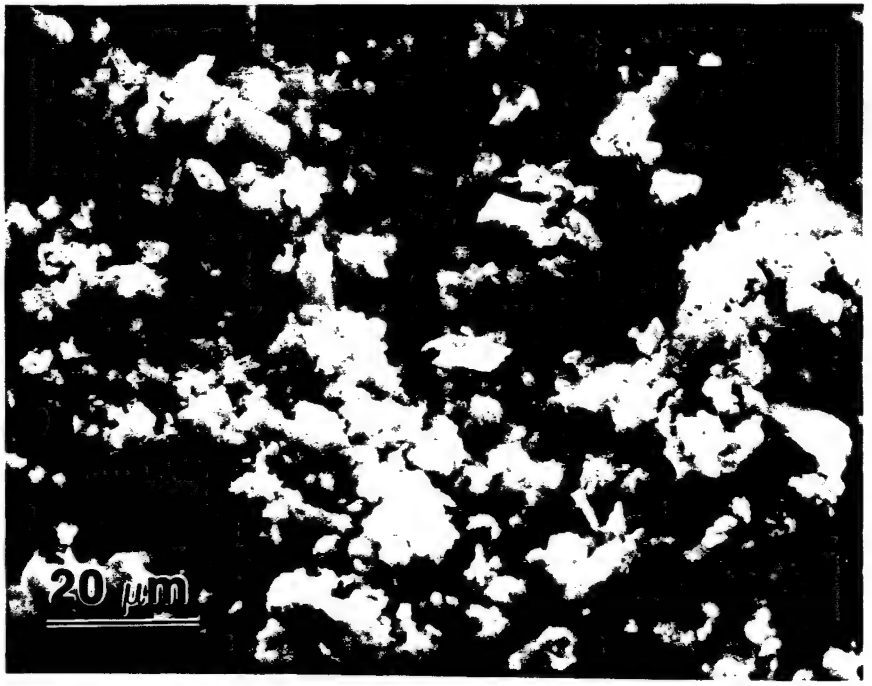

C

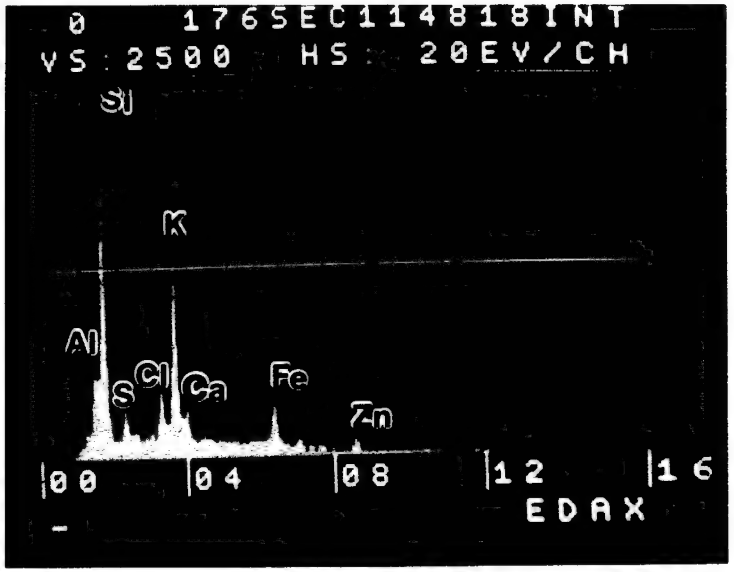

B

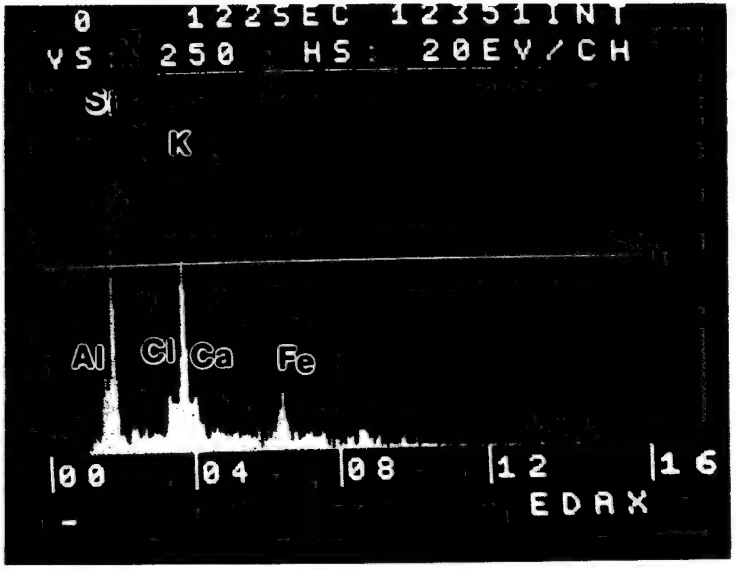

D

Figure F-3

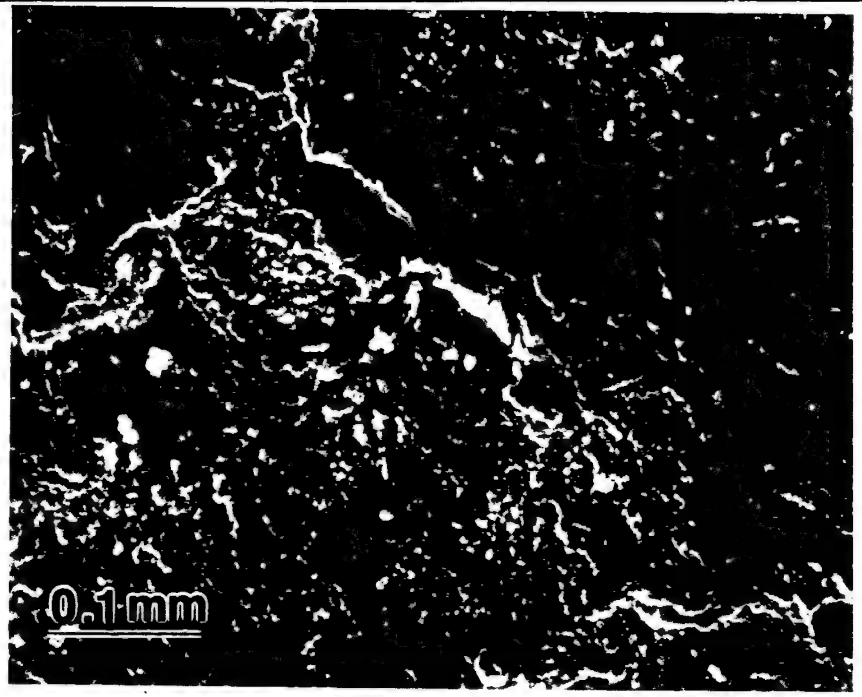

A

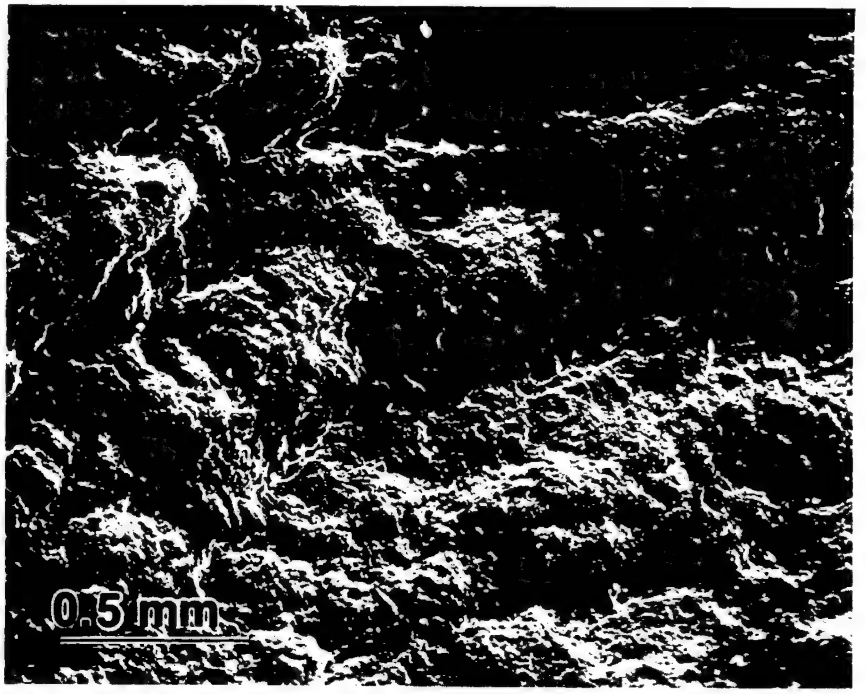

C

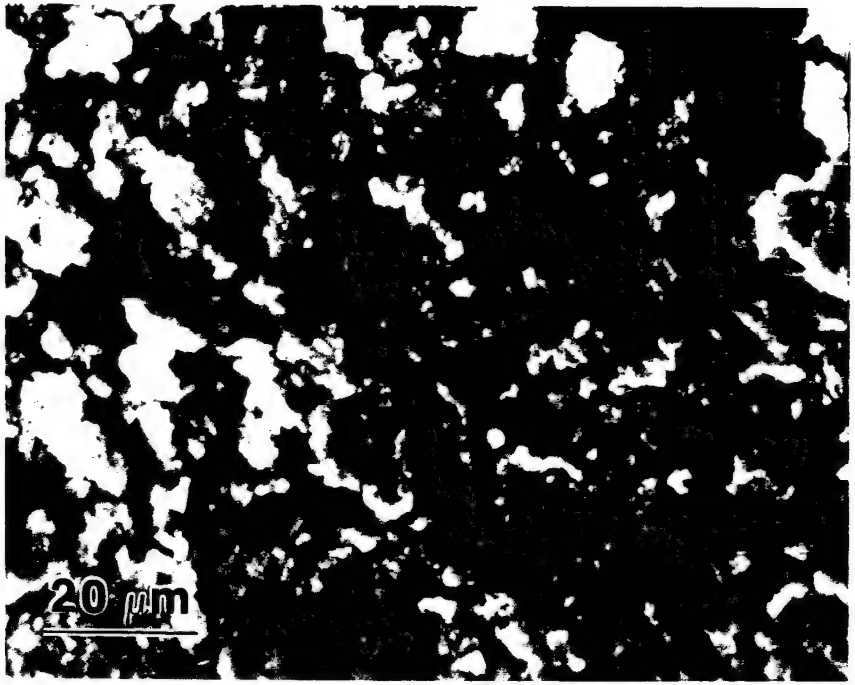

B

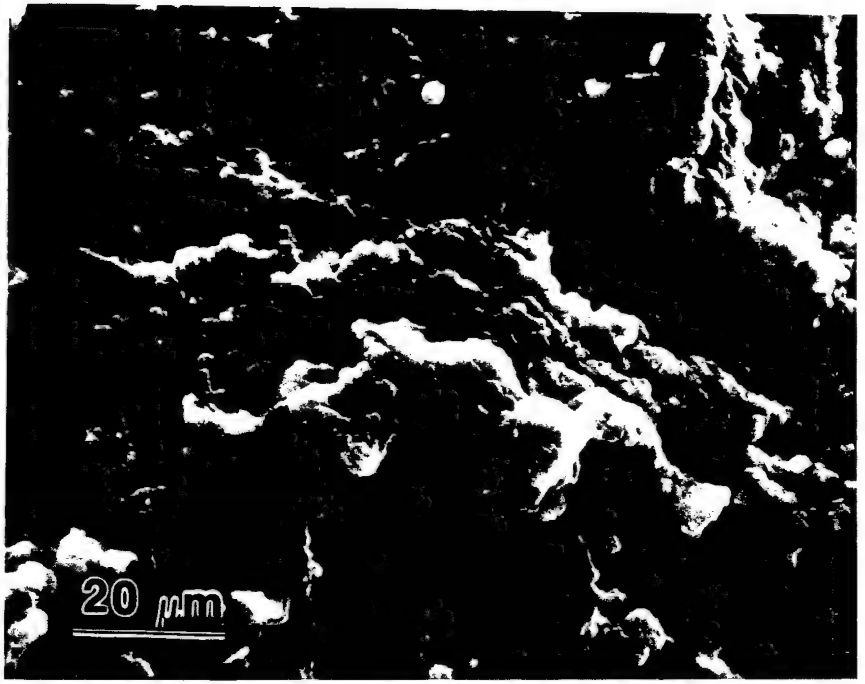

D

Figure F-4

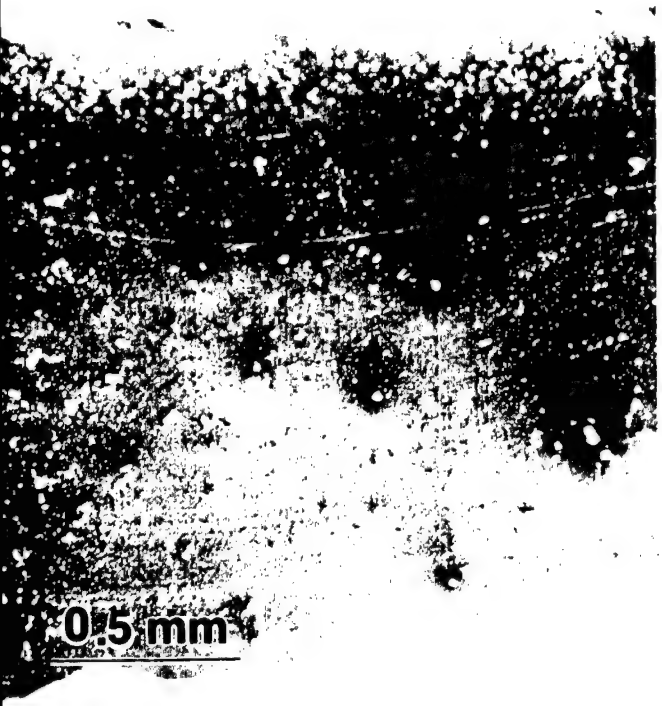

A

C

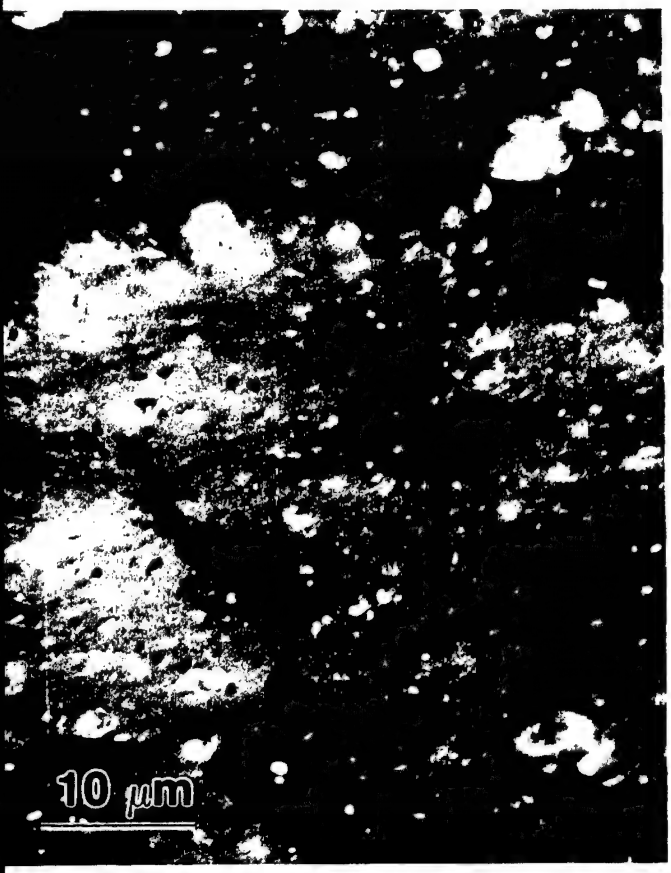

B

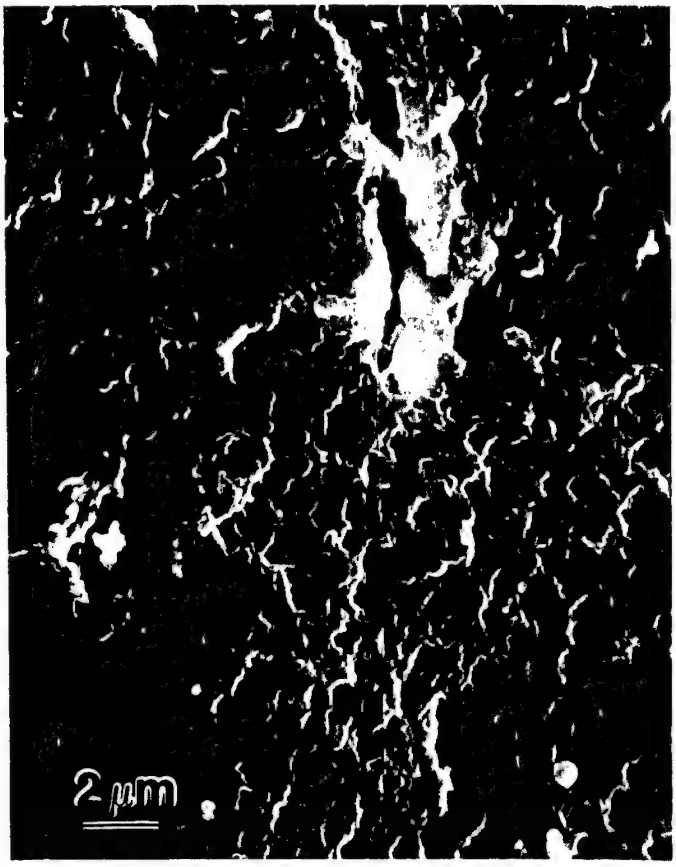

D

Figure F-5

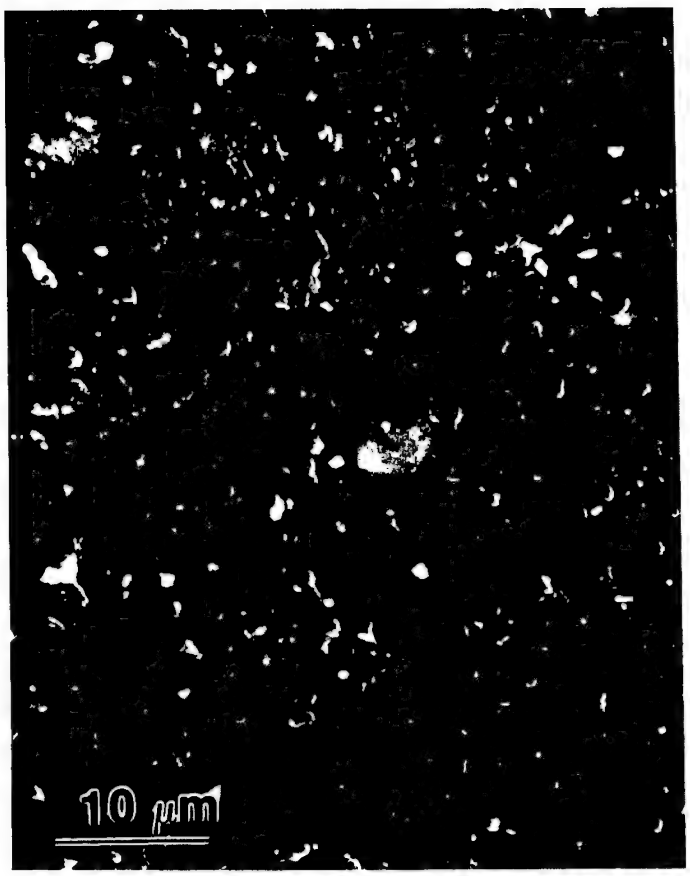

A

C

B

D

Figure F-6

APPENDIX G

Field Weight Loss

Field Weight Loss

In order to compare the performance of different track pads the reduction of pad thickness was used to characterize the relative performance of service pads received from YPG before the field weight loss data was obtained. Later, the apparent weight loss of service pad vs preservice pad "as received" was used in comparison (Table G-1).

Previous calculation of track pad service wear, based upon the apparent weight losses in the data lists provided by Mr. Jacob Patt, seems to indicate weight loss of track pads is relatively small (Table G-2) and the performance of T97E2 type pad is better. However, based upon the service weight loss of the rubber only, several meaningful results are revealed. The T97E2 pads with different geometry actually show no particular advantage in wear resistance. Commonly, their weight losses lie between the average and the lowest weight losses of T142 pads (Figures G-1 to G-3). For all the test courses (Figures G-4 to G-6), Firestone Experimental (FM) pads consistently show the lowest service weight loss, and Monarch pads have the highest weight loss except in the paved course where they are second to Firestone Triblend (FT) pads. Also noticed are the order of performance from good to poor is generally consistent. In details, the trend in cross-country and gravel courses is the same, yet in the paved course, GS pads performance is only inferior to FM pads, while they are second to last in both other courses. Pad wear on the paved course is slower at the beginning and faster in the last 500 miles of service. Conversely, both cross-country and gravel courses are fast at the beginning and slow down at the later stage of service (Figures G-7 to G-9). By using % weight loss per 250 miles of service as a measure of the rate of

pad deterioration, the pad wear rate is 4 to 8% on the paved course, 8 to 15% on gravel and 30 to 45% in cross-country service. Comparison of the performance of pads from the same manufacturer is also shown (Figures G-10 to G-18).

TABLE G-1

TRACK PAD WEAR

		GS	GK	FS	FK	SP
Original Height (cm)		2.34	2.40	2.46	2.34	2.67
Average % wear after	500 miles	33	26	30	36	23
	1000 miles	44	53	60	49	32
	1500 miles	69	73	70	72	52
Original Weight (gm)		2340	2305	2370	2370	2305
% weight loss after	500 miles	5.3	3.5	5.1	6.9	5.2
	1000 miles	17.5	13.9	14.8	17.7	14.5
	250 miles (cross country)	33.6	23.2	24.1	13.3	$\frac{29.0*}{13}$

*Two Std. Product pads were found in the cross-country pads.

TABLE G-2

Effect of Pad Type on Weight Loss During Field Testing

Pad Type	# of Final Weight Loss Data	Average (%)
Monarch*	2	34.5
FT**	2	30.2
GS	3	28.6
GK	3	28.5
FK	3	26.2
FA***	2	26.0
STD	3	24.8
FS	3	24.0
FM	3	21.5

* X-country weight loss not shown

** Gravel course weight loss not shown

*** Paved course weight loss not shown

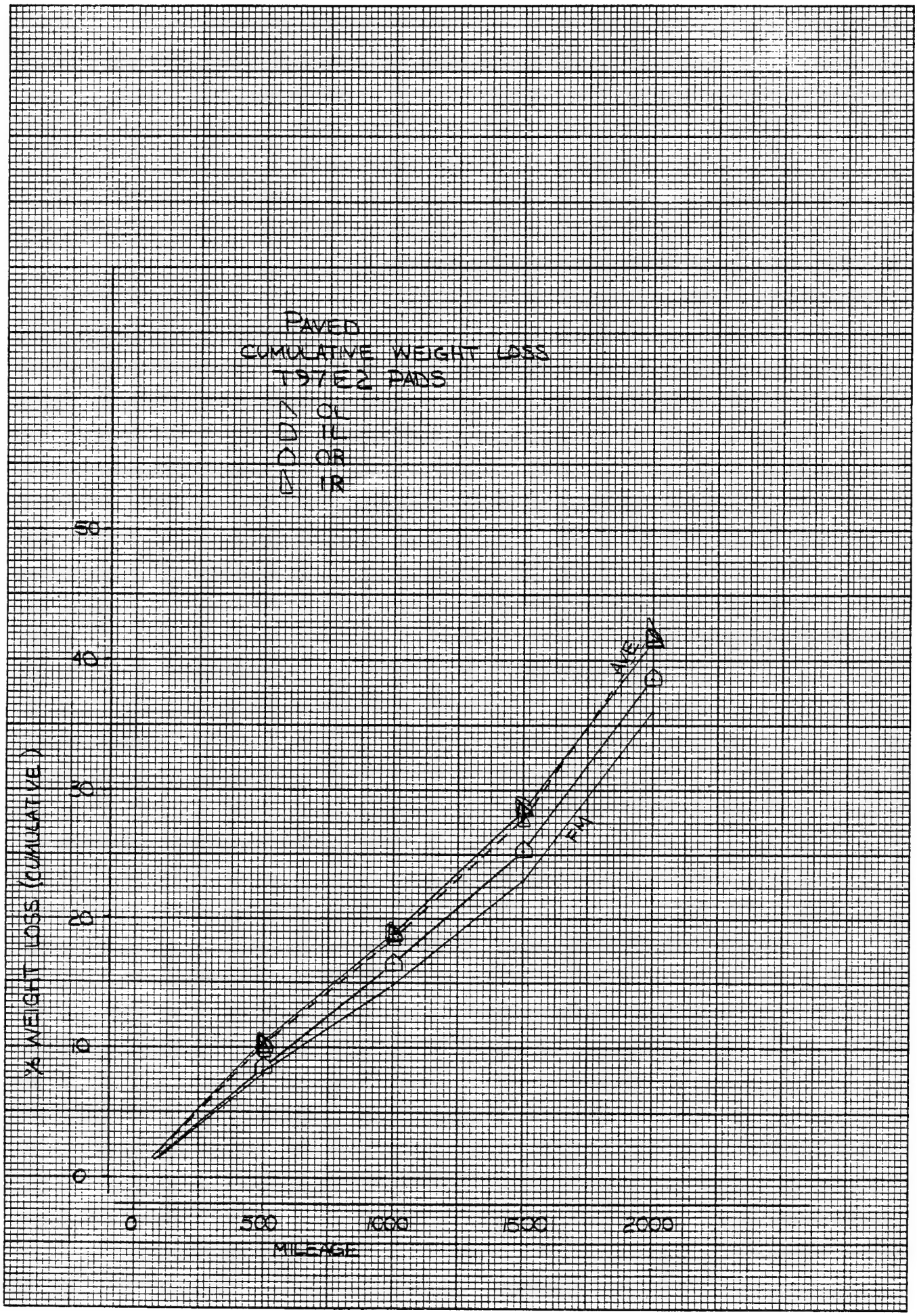
PAVED
CUMULATIVE WEIGHT LOSS
T57E2 PADS
OL
IL
OR
IR
AVE
% WEIGHT LOSS (CUMULATIVE)
50
40
30
20
10
0
0
500
1000
1500
2000
MILEAGE

Figure G-1

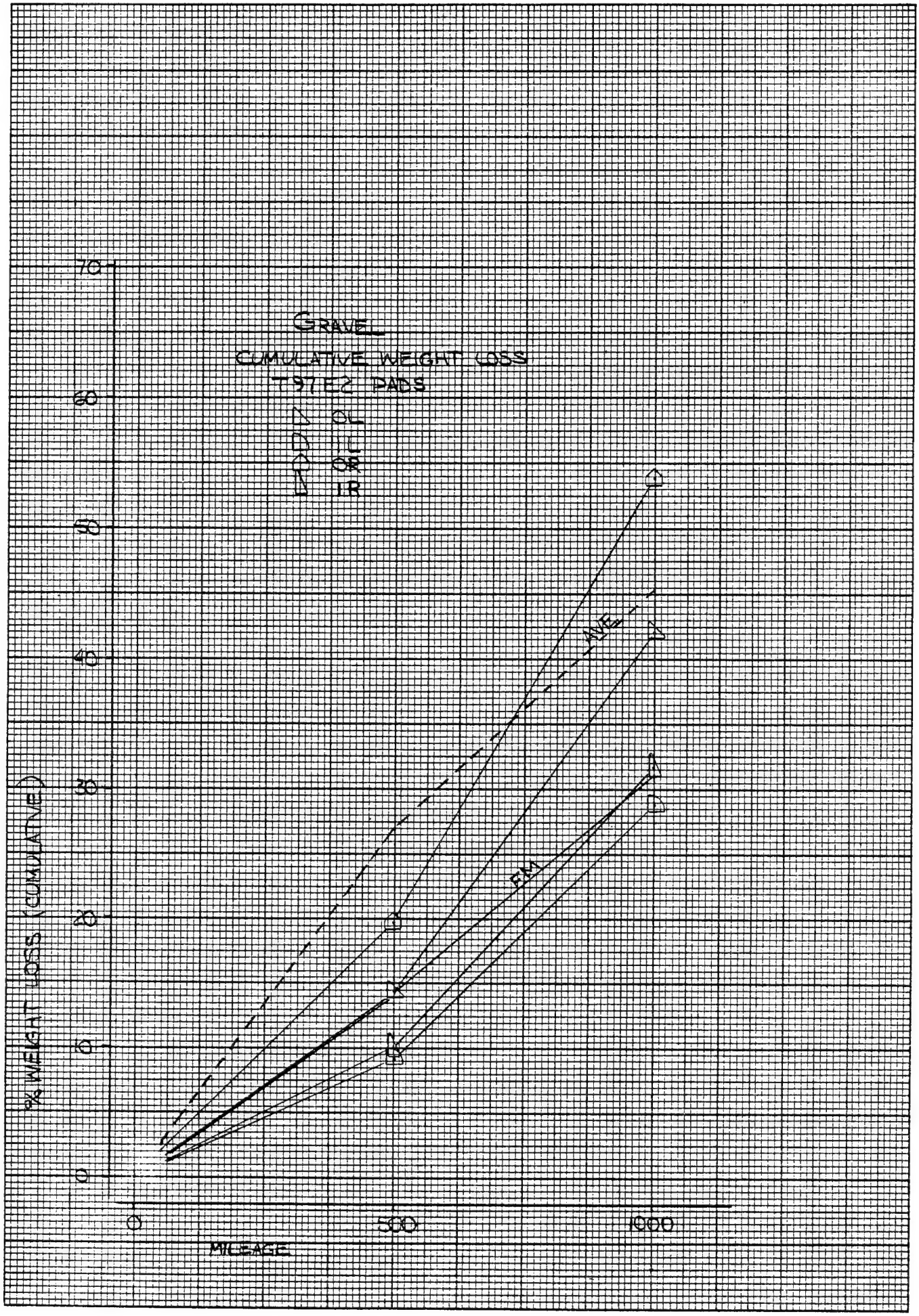
GRAVEL
CUMULATIVE WEIGHT LOSS
TEST 2 PADS
OL
IL
OR
IR
% WEIGHT LOSS (CUMULATIVE)
MILEAGE
0
500
1000
70
60
50
40
30
20
10
0
FWE
FM

Figure G-2

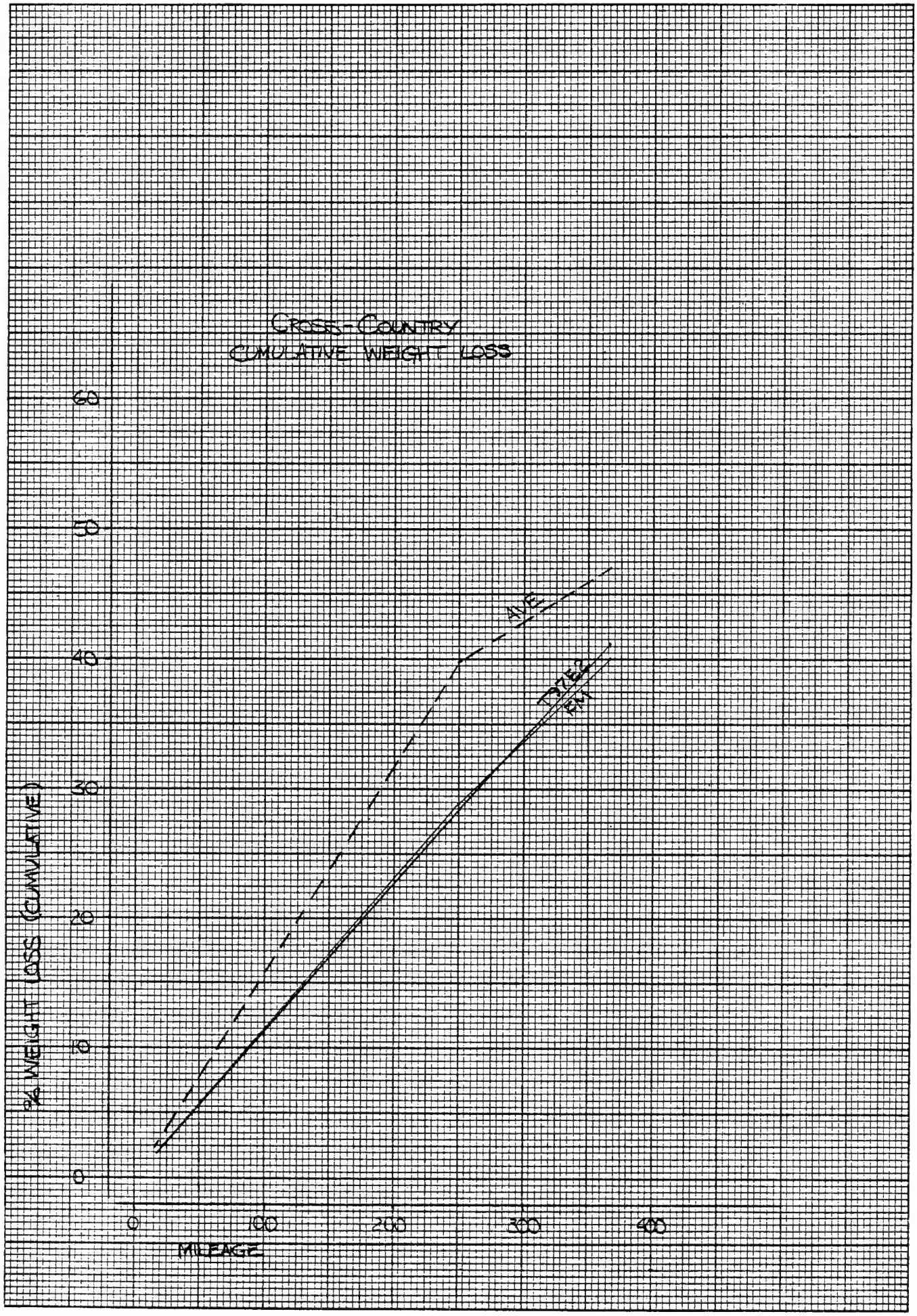
CROSS-COUNTRY
CUMULATIVE WEIGHT LOSS
60
50
40
30
20
10
0
% WEIGHT LOSS (CUMULATIVE)
0
100
200
300
400
MILEAGE
AVE
TYLER
FAT

Figure G-3

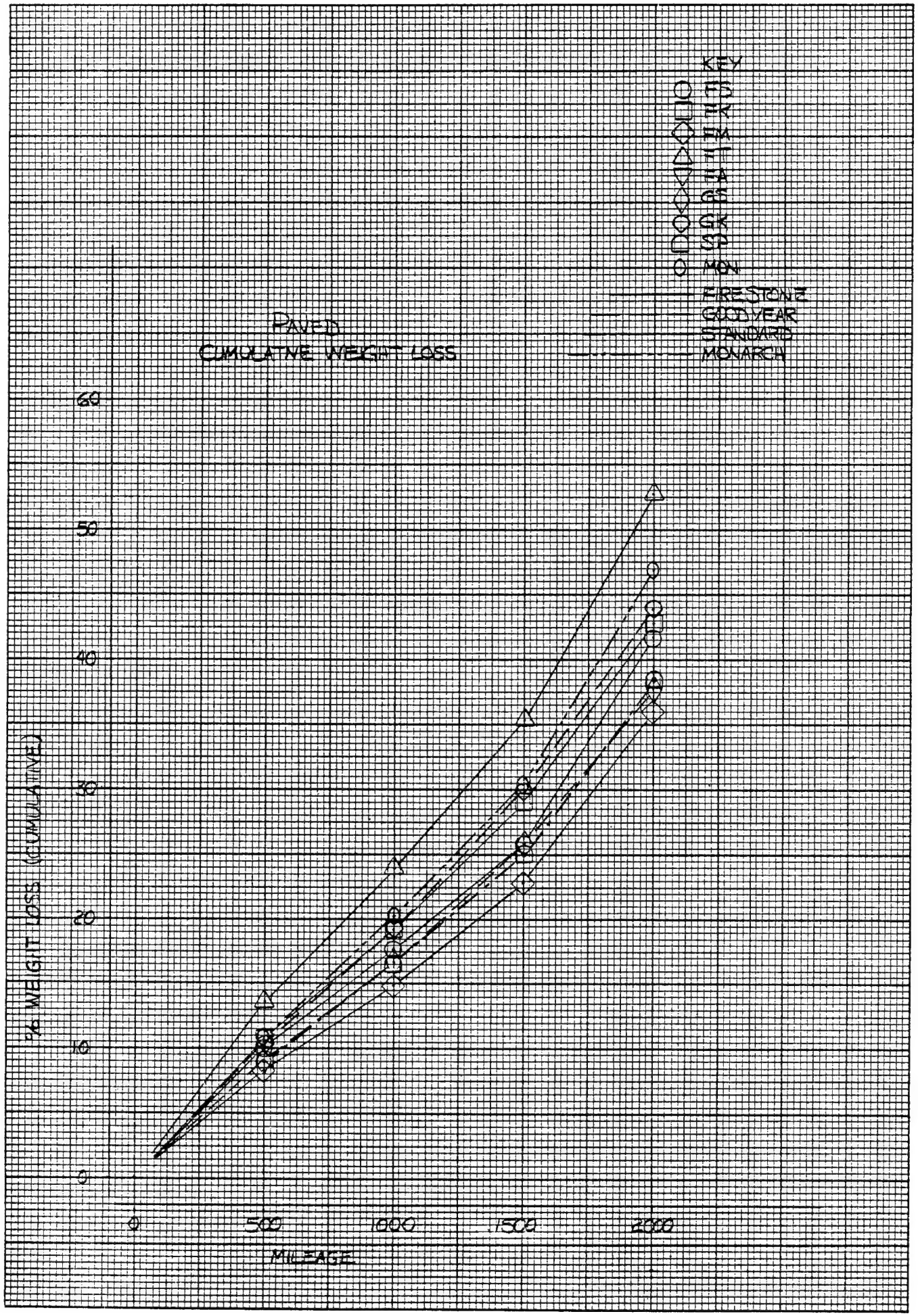
KEY
FS
GK
FM
FA
GS
GK
SP
MON
FIRESTONE
GOODYEAR
STANDARD
MONARCH
PAVED
CUMULATIVE WEIGHT LOSS
% WEIGHT LOSS (CUMULATIVE)
60
50
40
30
20
10
0
0
500
1000
1500
2000
MILEAGE

Figure G-4

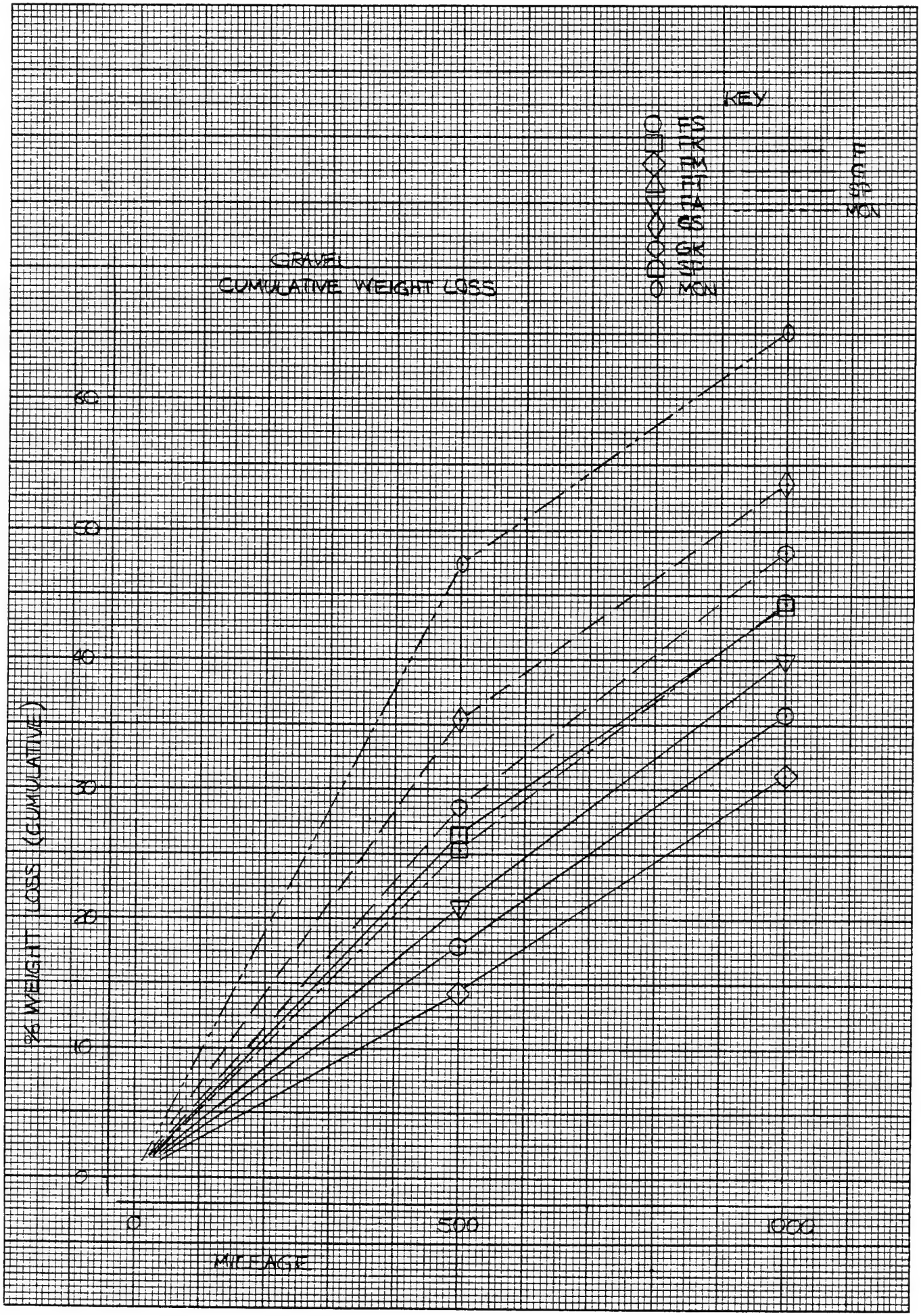
KEY
FS
KM
TT
GS
GK
SF
MON
GRAVEL
CUMULATIVE WEIGHT LOSS
% WEIGHT LOSS (CUMULATIVE)
60
50
40
30
20
10
0
0
500
1000
MILEAGE

Figure G-5

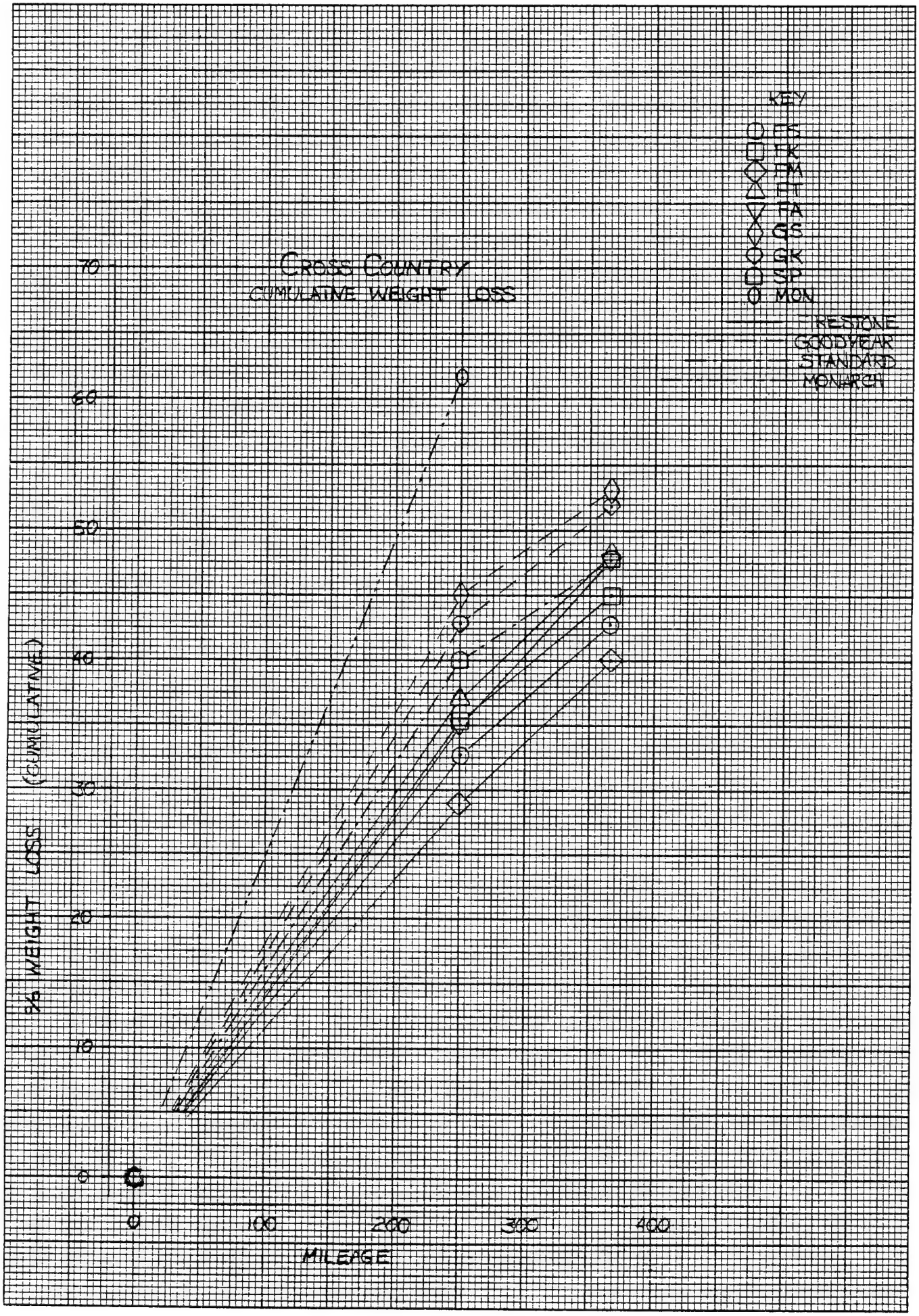
CROSS COUNTRY
CUMULATIVE WEIGHT LOSS
KEY
FS
FK
FM
FT
FA
GS
GK
SP
MON
RESTONE
GOODYEAR
STANDARD
MONARCH
% WEIGHT LOSS (CUMULATIVE)
70
60
50
40
30
20
10
0
0
100
200
300
400
MILEAGE

Figure G-6

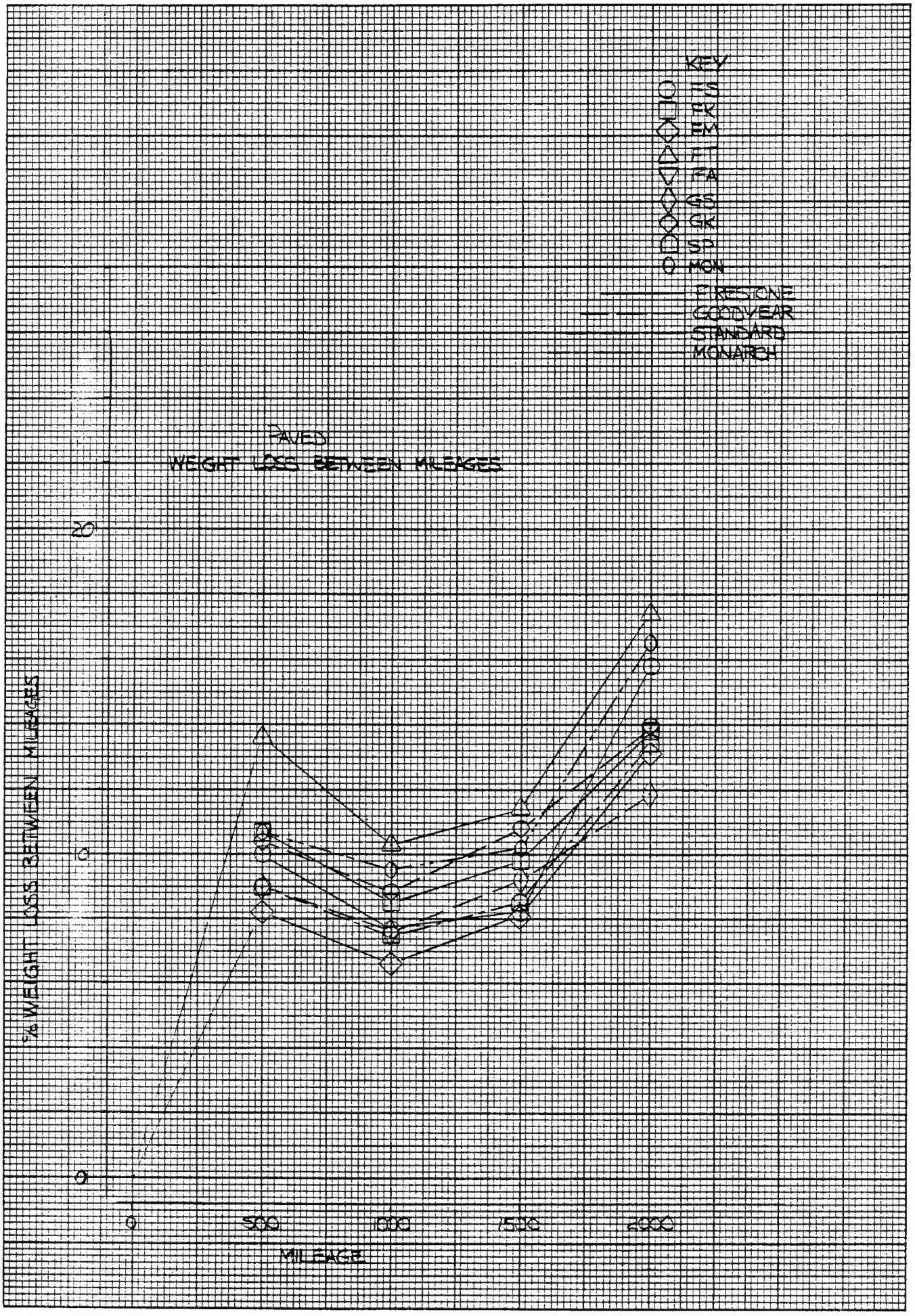
KEY
FS
FK
EM
FT
FA
GS
GK
SP
MON
FIRESTONE
GOODYEAR
STANDARD
MONARCH
PAVED
WEIGHT LOSS BETWEEN MILEAGES
% WEIGHT LOSS BETWEEN MILEAGES
20
0
500
1000
1500
2000
MILEAGE

Figure G-7

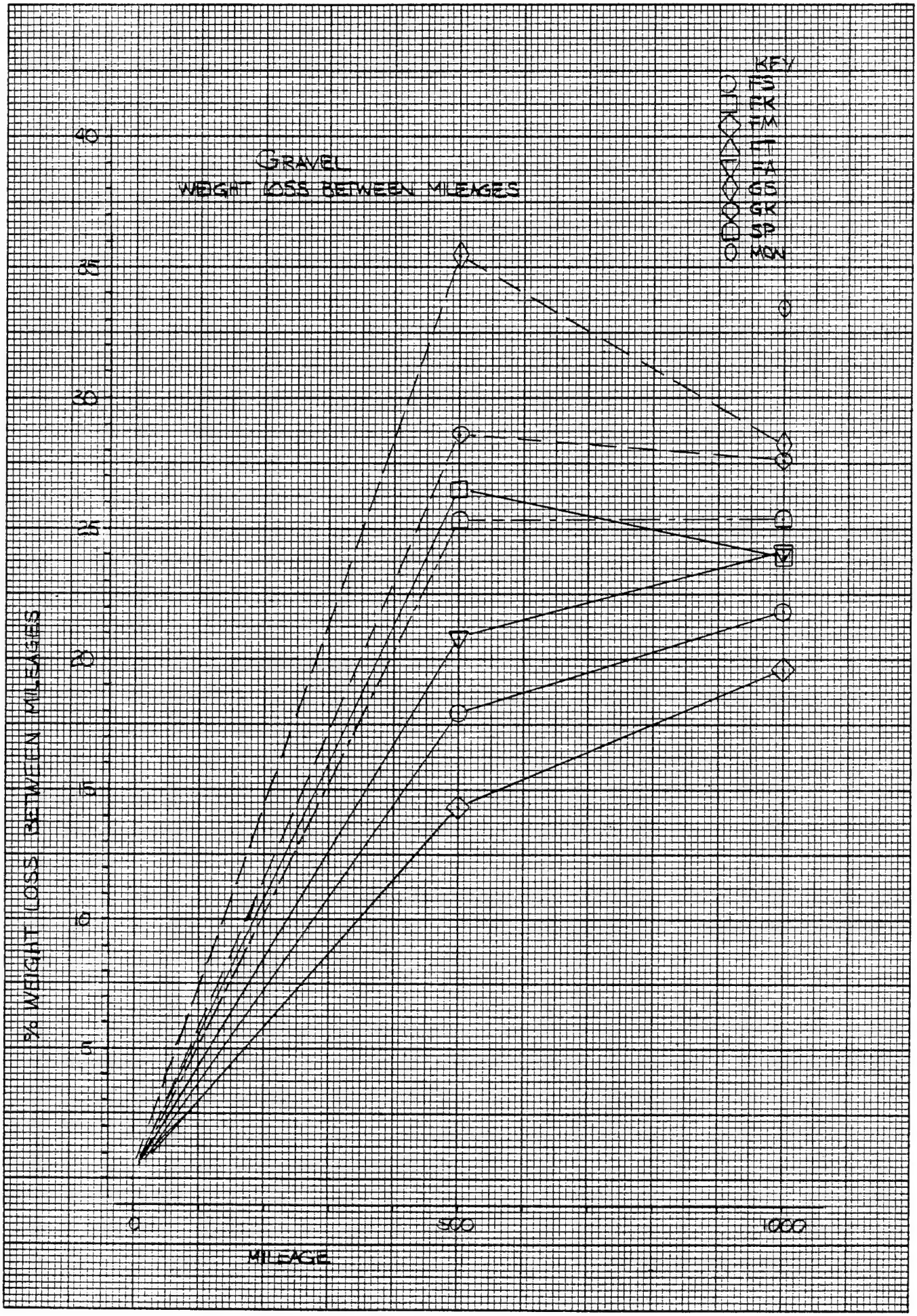
GRAVEL
WEIGHT LOSS BETWEEN MILEAGES
KEY
FS
FK
FM
FT
FA
GS
GR
SP
MON
40
35
30
25
20
15
10
5
0
% WEIGHT LOSS BETWEEN MILEAGES
0
500
1000
MILEAGE

Figure G-3

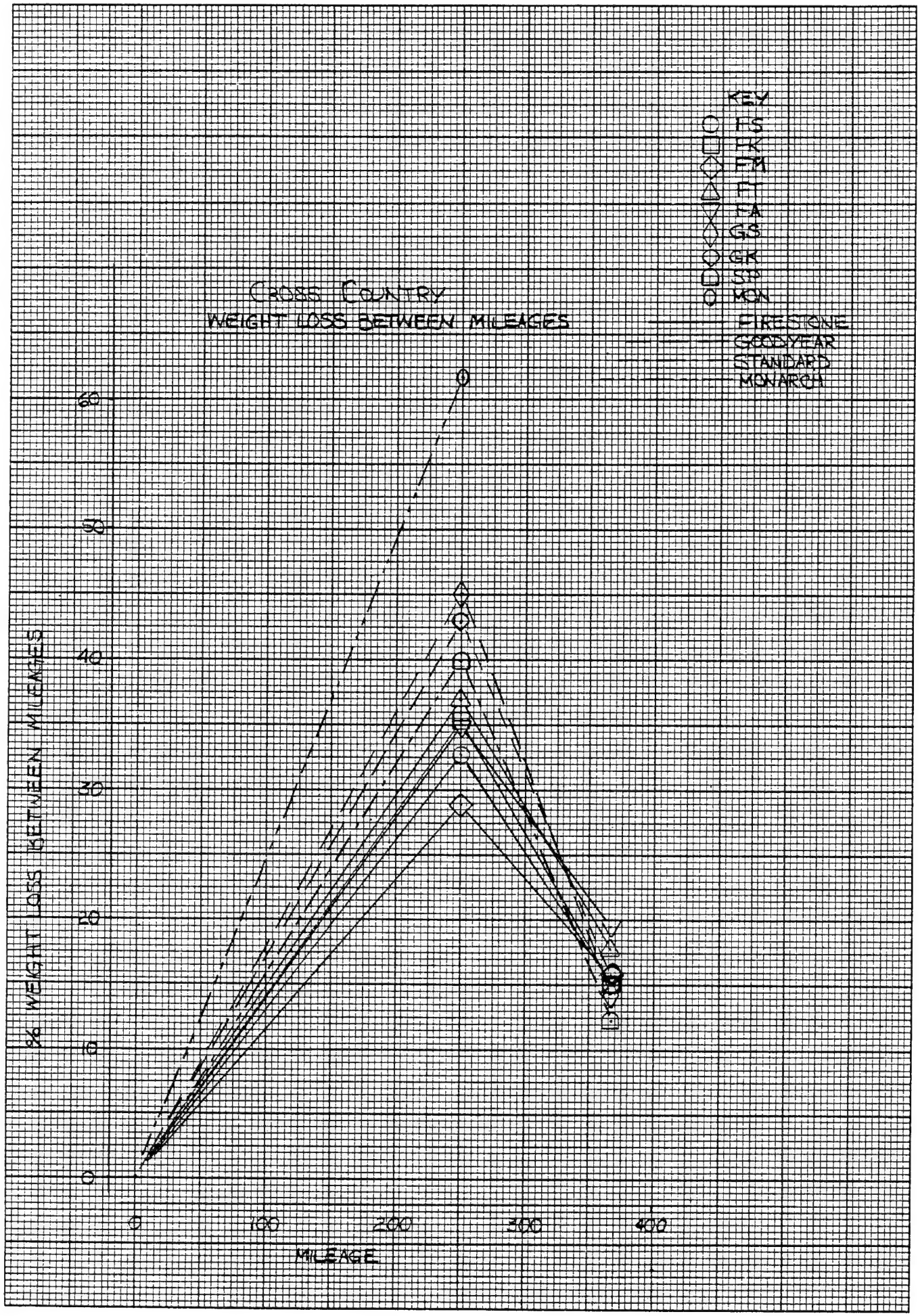
CROSS COUNTRY
WEIGHT LOSS BETWEEN MILEAGES
KEY
FS
FK
FM
FT
FA
GS
GK
SP
MON
FIRESTONE
GOODYEAR
STANDARD
MONARCH
% WEIGHT LOSS BETWEEN MILEAGES
0
10
20
30
40
60
0
100
200
300
400
MILEAGE

Figure G-9

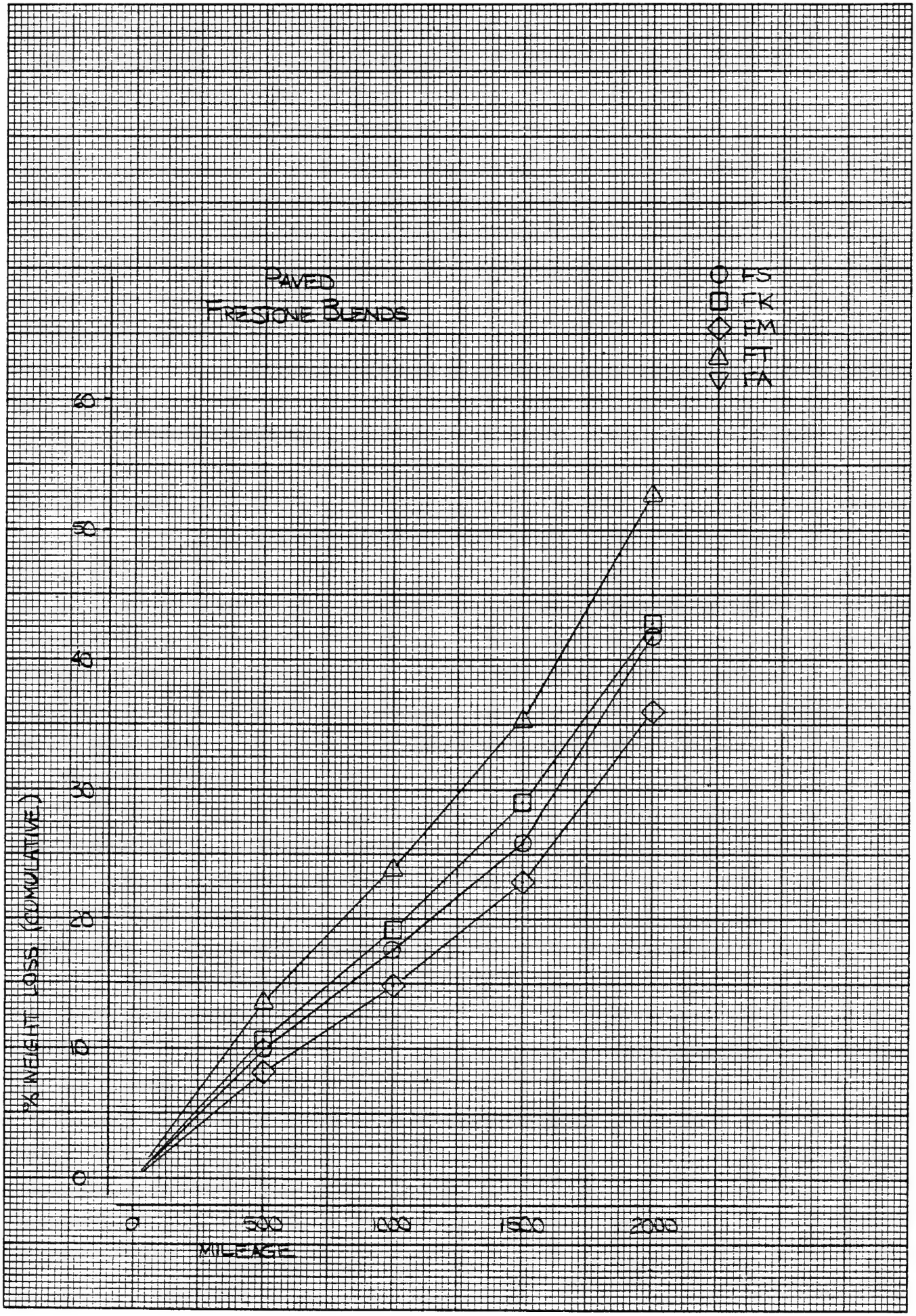
PAVED
FIRESTONE BLENDS
FS
FK
FM
FT
FA
% WEIGHT LOSS (CUMULATIVE)
0
10
20
30
40
50
60
0
500
1000
1500
2000
MILEAGE

Figure G-10

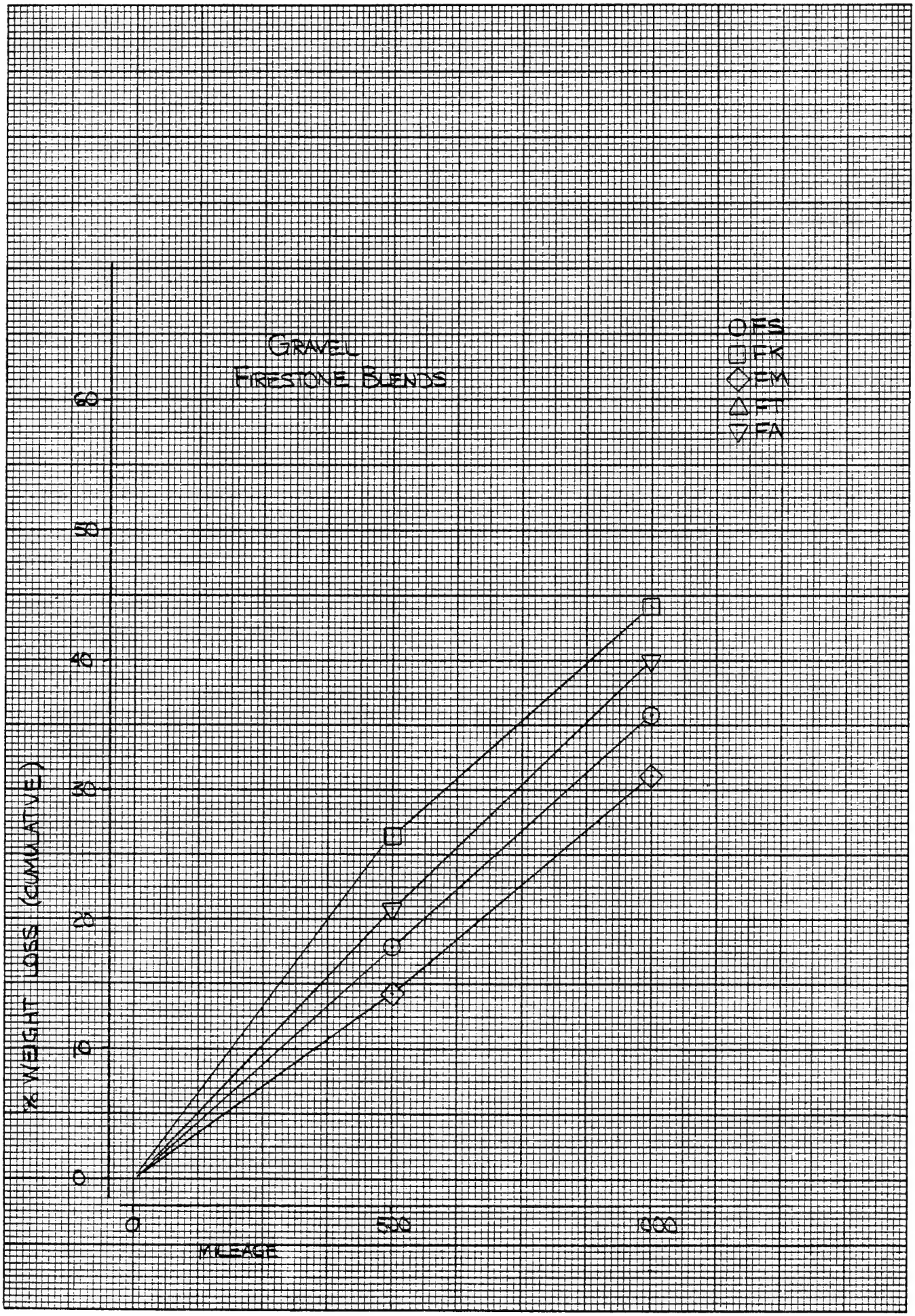
GRAVEL
FIRESTONE BLENDS
FS
FK
FM
FT
FA
% WEIGHT LOSS (CUMULATIVE)
60
50
40
30
20
10
0
0
500
1000
MILEAGE

Figure G-11

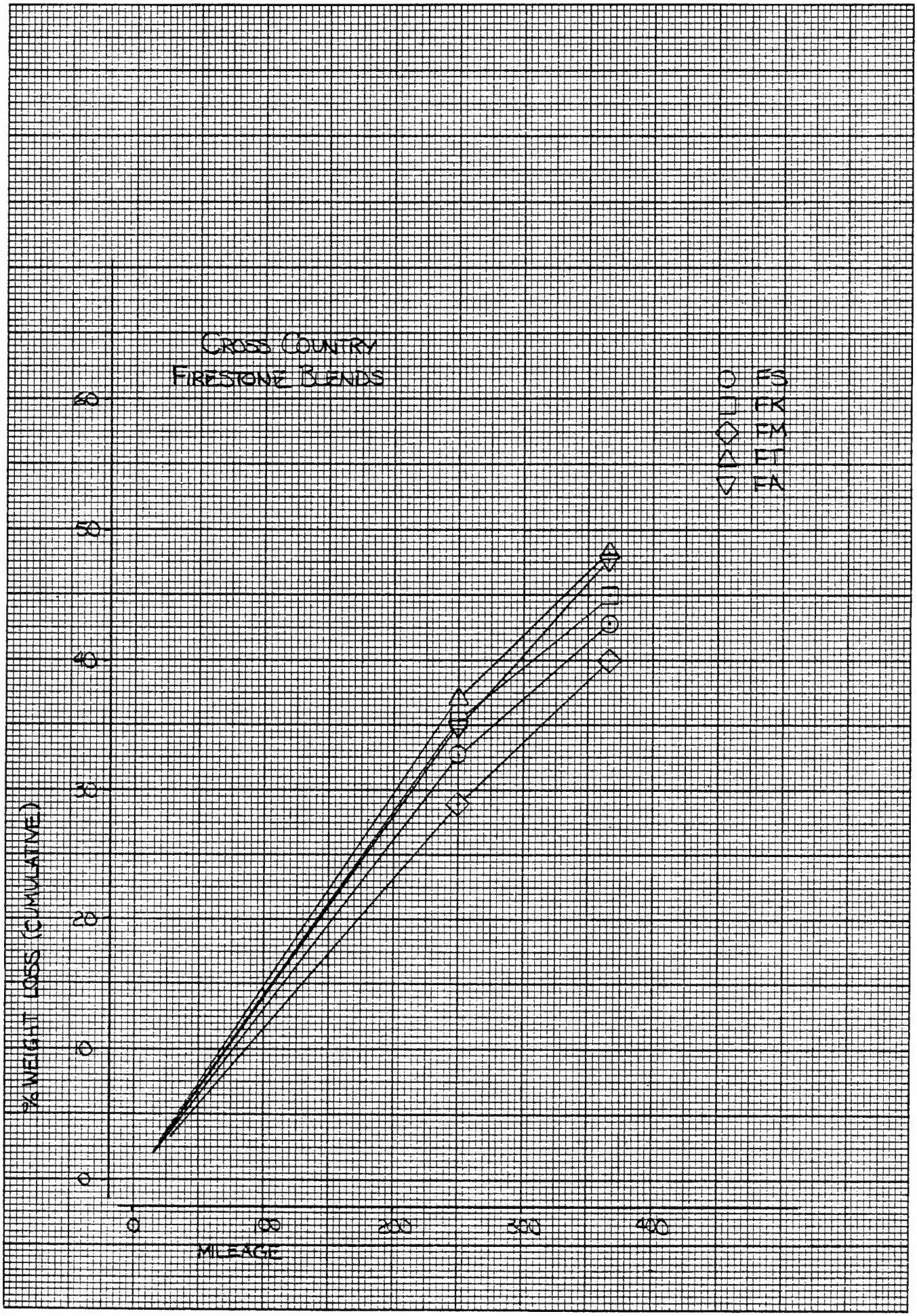
CROSS COUNTRY
FIRESTONE BLENDS
FS
FK
FM
FT
FA
% WEIGHT LOSS (CUMULATIVE)
60
50
40
30
20
10
0
0
100
200
300
400
MILEAGE

Figure G-12

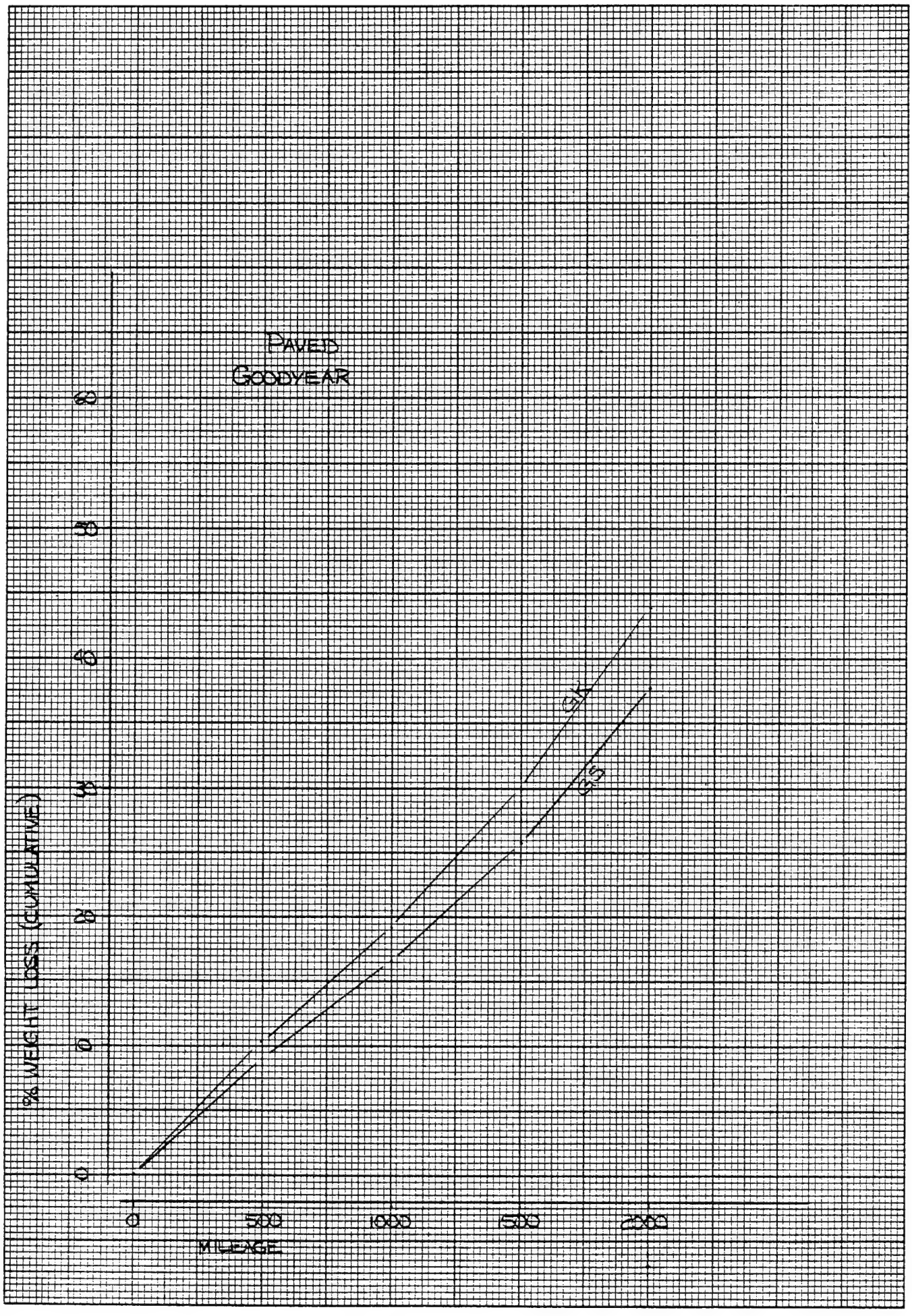
PAVED
GOODYEAR
60
50
40
30
20
10
0
% WEIGHT LOSS (CUMULATIVE)
0
500
1000
1500
2000
MILEAGE
54
53

Figure G-13


GRAVEL
GOODYEAR
GS
GT
% WEIGHT LOSS (CUMULATIVE)
0
10
20
30
40
50
60
0
500
1000
MILEAGE

Figure G-14

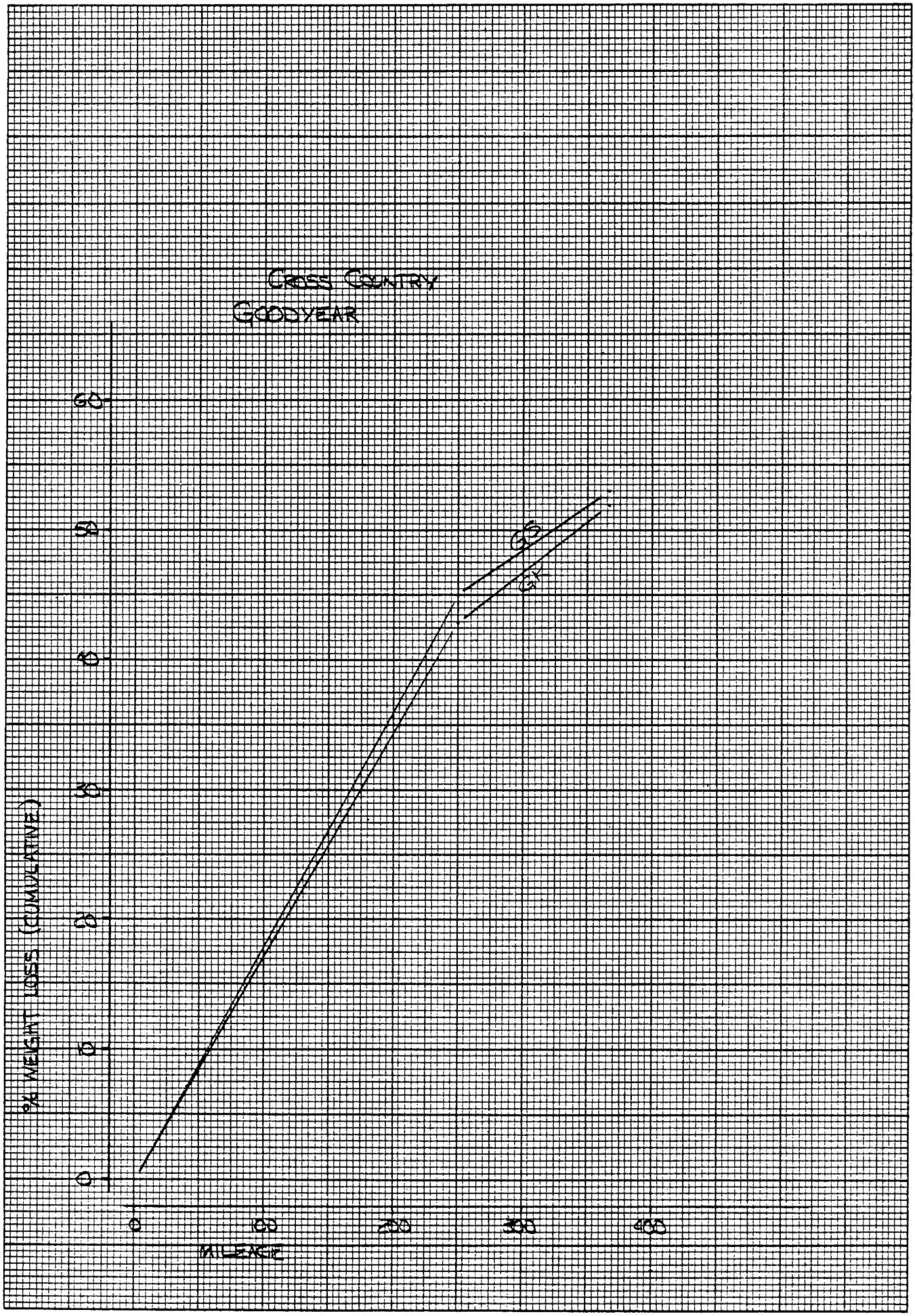
CROSS COUNTRY
GOODYEAR
60
50
40
30
20
10
0
% WEIGHT LOSS (CUMULATIVE)
0
100
200
300
400
MILEAGE
GS
GX

Figure G-15

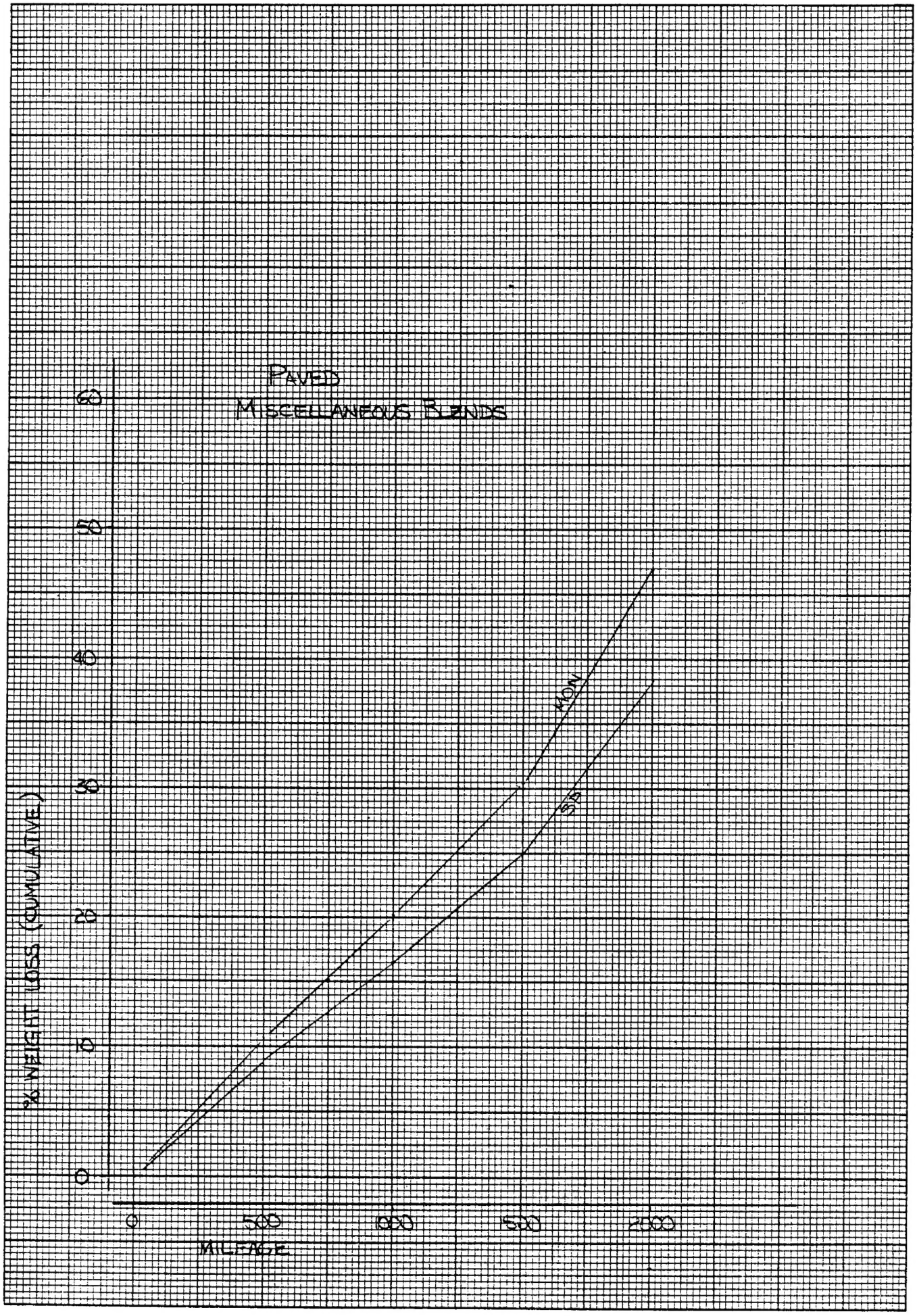
PAVED
MISCELLANEOUS BLENDS
% WEIGHT LOSS (CUMULATIVE)
0
10
20
30
40
50
60
0
500
1000
1500
2000
MILEAGE
HOW
STS

Figure G-16

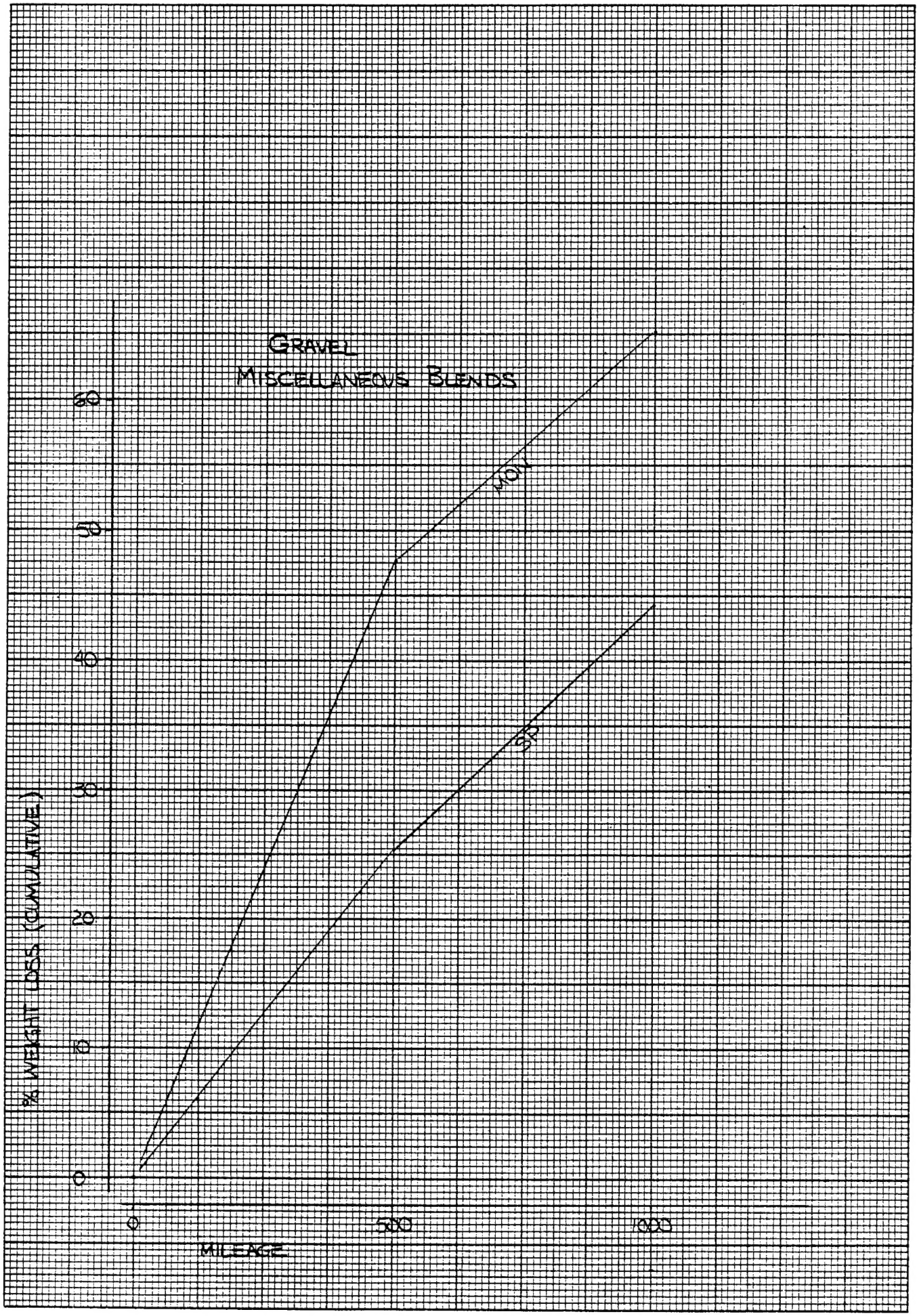
GRAVEL
MISCELLANEOUS BLENDS
MDH
SD
% WEIGHT LOSS (CUMULATIVE)
0
10
20
30
40
50
60
0
500
1000
MILEAGE

Figure G-17

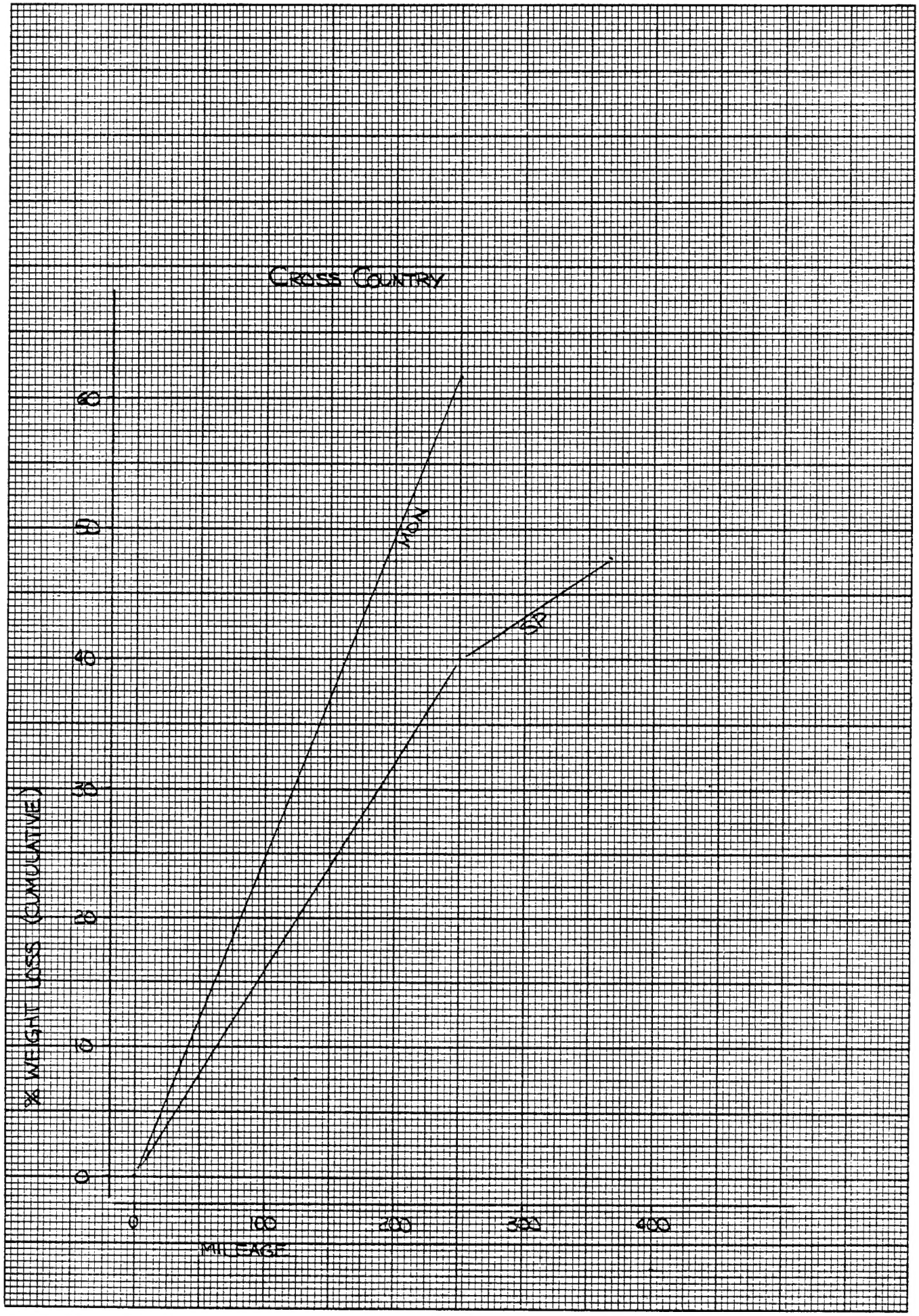
CROSS COUNTRY
% WEIGHT LOSS (CUMULATIVE)
0
10
20
30
40
50
60
MILEAGE
0
100
200
300
400
NON
SP

Figure G-18